Int J Earth Sciences (Geol Rundsch) (2001) 90:304–324
DOI 10.1007/s005310000139

ORIGINAL PAPER

A. Kröner · P. Jaeckel · E. Hegner · M. Opletal

Single zircon ages and whole-rock Nd isotopic systematics of early Palaeozoic granitoid gneisses from the Czech and Polish Sudetes (Jizerské hory, Krkonoše Mountains and Orlice-Sněžník Complex)

Received: 15 July 1999 / Accepted: 28 August 2000 / Published online: 9 March 2001

Abstract Granitoid orthogneisses make up the predominant rock type in the West Sudetes from Jizerské hory in the NW to the Orlické hory and Sněžník Mountains in the SE. These generally strongly foliated gneisses are calc-alkaline in composition and display trace element characteristics suggesting generation in a volcanic arc setting. Single zircon ages reflecting the time of emplacement of the gneiss protoliths define a relatively narrow Cambro-Ordovician range between 502 and 515 Ma. This is similar to previously reported zircon ages from the Czech and Polish West Sudetes and documents an important and regionally extensive post-Cadomian magmatic event that we relate to continental arc magmatism on the margin of Avalonia that developed during closure of the Tornquist Ocean. An age of 492 Ma for a microgranite dyke cutting deformed and metamorphosed orthogneisses in the Orlické hory shows the main deformation to be early Paleozoic. Zircon xenocryst minimum ages range between 546 and 2070 Ma and show maxima in the Cadomian/Pan-African (550–850 Ma) and Grenvillian (1000–1300 Ma) time brackets. The Grenvillian event is also evident from Nd mean crustal residence ages that vary between 1.34 and 1.87 Ga. From these data we suggest that the pre-Variscan granitoid gneisses of the Czech West Sudetes were largely generated by melting of a predominantly Grenville-age basement that was part of the northern margin of Gondwana and may have been related to Grenville-age basement now identified in northern South America.

Keywords Avalonia · Granitoid gneisses · Nd isotopes · Sudetes · Zircon · Geochronology

A. Kröner (✉) · P. Jaeckel
Institut für Geowissenschaften, Universität Mainz,
55099 Mainz, Germany
E-mail: kroener@mail.uni-mainz.de
Phone: +49-6131-3922163
Fax: +49-6131-3924769

P. Jaeckel
Max-Planck-Institut für Chemie, Postfach 3060, 55020 Mainz, Germany

E. Hegner
Institut für Mineralogie, Petrologie und Geochemie, Universität Tübingen, Wilhelmstrasse 56, 72074 Tübingen, Germany

M. Opletal
Czech Geological Survey, Klárov 3, 11821 Praha 1, Czech Republic

Present address:
E. Hegner
Institut für Mineralogie, Universität München, Theresienstrasse 41, 80333 München, Germany

Introduction

The Sudetes Mountains in the Czech Republic and Poland define the NE part of the Bohemian Massif and are dominated by a varied rock suite which consists of different types of granites, orthogneisses, blastomylonites and migmatites (hereafter collectively named garnitoid gneisses). These rocks occur predominantly in the Jizerské Mountains, in the southern part of the Krkonoše Mountains, and in the Orlické hory which is part of the Orlice-Sněžník Complex (Fig. 1). Their genesis has been discussed by many authors such as Bederke (1929, 1943), Fischer (1935), Opletal et al. (1980), Don et al. (1990), Oliver et al. (1993) and Cymerman (1997), and the majority of authors concluded that the orthogneiss precursors were of magmatic origin. Transformation of sedimentary rocks into the granitoid gneisses by processes of metasomatism has also been considered (e.g., Smulinowski 1979) but is incompatible with field evidence (Bederke 1943; Opletal et al. 1980; Don et al. 1990) and zircon morphology as demonstrated herein. Opinions vary as to the age of these gneisses, suggesting Cadomian (Bederke 1956; Mísař 1963; Oberc 1969, 1972; Domečka 1970; Mísař et al. 1983; Chaloupský 1989; Svoboda et

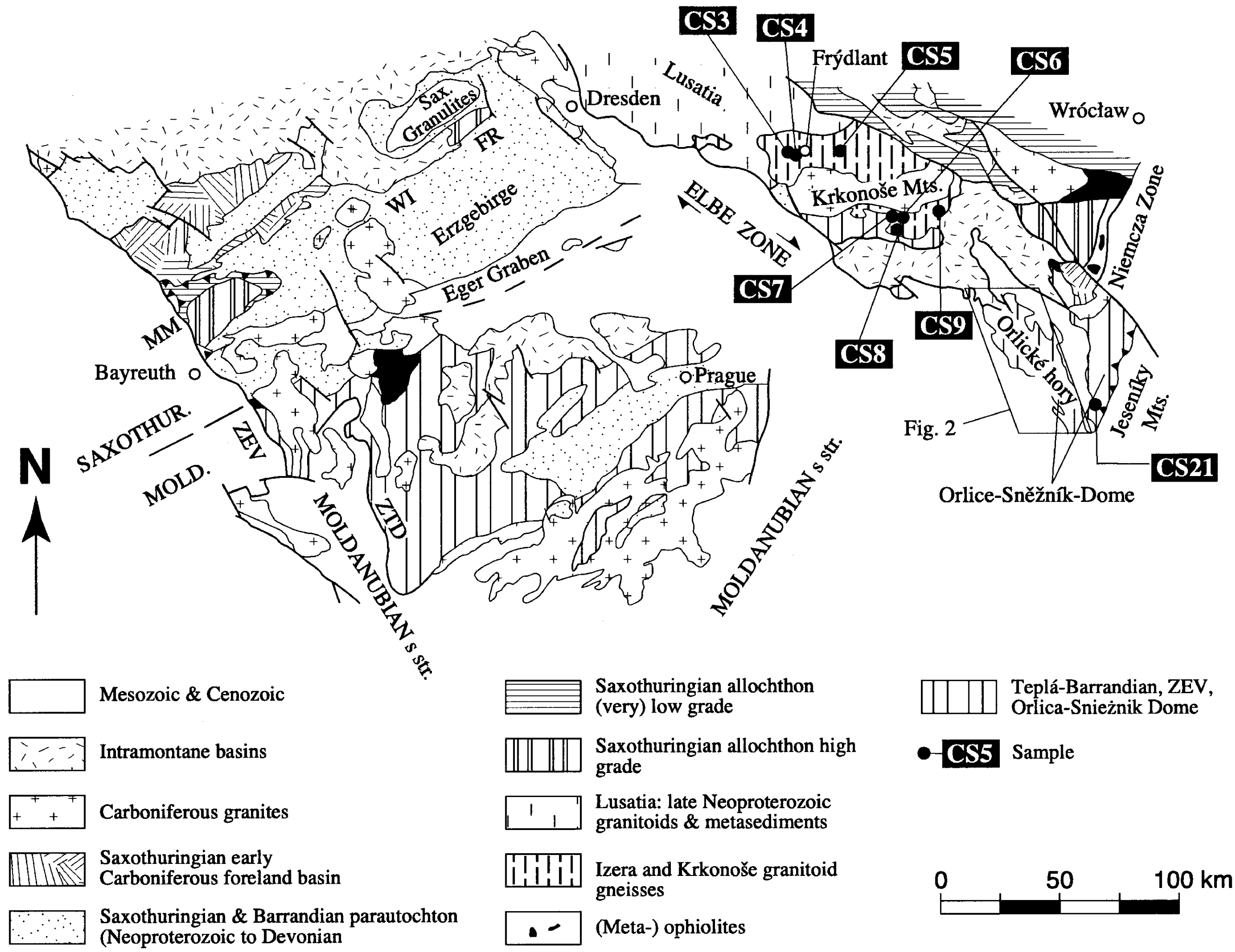

Fig. 1 Schematic and simplified geological map showing major rock units of the Bohemian Massif and sample locations in the Jizerské hory and Krkonoše Mountains, Czech West Sudetes. (Modified after Dörr et al. 1998)

al. 1966; Suk et al. 1984), Caledonian (e.g., Bederke 1925, 1929; Fischer 1935; Domečka 1970), Don et al. 1990; Oliver et al. 1993), or Variscan ages (Don 1964; Dumicz 1979, 1991; Cymerman 1992; Bakun-Czubarow 1992, 1993). Our study is concerned with the primary ages and tectonic setting of the gneiss protoliths and with Nd mean crustal residence ages of these rocks which may help to constrain their evolution.

Summary of regional geology and tectonic evolution

The Sudetes are situated NE of the Elbe Zone lineament (Fig. 1) and are subdivided into the West Sudetic and East Sudetic parts (Bederke 1929) or into the Lugicum and Silesicum (Suess 1912). The NW part is made up of the Lusatian Massif (hereafter LM), predominantly encompassing granitoids of Cadomian (540–580 Ma) and minor Variscan (~304 Ma) age (Kröner et al. 1994a). The LM belongs to the lowest erosion level of the entire area and may have acted as an autochthon for the thrust sheets carrying the orthogneisses of the Jizera complex. Cymerman et al. (1997) have interpreted the West Sudetes in terms of the terrane concept.

The Jizera Gneiss (Izera in the Polish literature) constitutes a broad E/W-trending belt around and east of Frýdlant in the Czech Republic and extending into Poland (Fig. 1). It is a coarse-grained porphyritic granite to porphyroblastic granite-gneiss and has been described in detail by Domečka (1970) and Borkowska et al. (1980) who concluded that it evolved from a granitic precursor regionally known as Rumburk granite. Due to tectonometamorphic processes of varying intensity, various types of orthogneisses have developed via a metagranitic stage. Thinly laminated, almost mylonitic gneisses are one end member of this series. Blue quartz, which is a characteristic mineral of the Rumburk granite, also occurs locally in the Jizera orthogneisses, and a similar situation also applies to the Krkonoše orthogneisses, described by Chaloupský (1989), although this author assigned them to the

Cadomian orogen. The same model is applicable for similar rocks occurring in the Polish part of the Sudetes (Teisseyre 1973). Żelaźniewicz (1997) and Żelaźniewicz et al. (1998) have shown that the protolith of the Jizera Gneiss intruded into the 540- to 580-Ma-old Lusatian granitoid suite.

The Jizera Gneiss has variously been regarded to be of magmatic origin (Bederke 1939; Schwarzbach 1943; Watznauer 1955; Domečka 1970) or to have resulted from metasomatic transformation of Precambrian metasediments (Oberc 1961; Szałamacha and Szałamacha 1964). Precambrian as well as pre-Ordovician-Silurian crustal sources have been inferred (for references see Borkowska et al. 1980). Our own observations as well as the zircon morphology described herein and the geochemical data of Domečka (1970) and Borkowska et al. (1980) leave no doubt that the Jizera gneiss is derived from a calc-alkaline porphyritic granite which intruded into the 545- to 580-Ma-old Lusatian granites (Żelaźniewicz et al. 1998).

The genesis and age of granitoid orthogneisses in the Orlice-Sněžník Complex (OSC; Orlica-Śnieżnik in the Polish literature, Fig. 1) have been discussed by Bederke (1925, 1929), Fischer (1935), Opletal et al. (1980), Don et al. (1990), Oliver et al. (1993), Přikryl et al. (1996), and Cymerman (1997), as well as others. In general, two different orthogneiss types have been distinguished, namely a medium- to coarse-grained gneiss, which often shows augen structure and is named Sněžník gneiss (Schneeberggneis; Fischer 1935), and a fine-grained, mylonitic gneiss variety named Gierałtów gneiss (Gersdorfgneis; Fischer 1935) which often has a migmatitic appearance. Opletal et al. (1980) and Turniak et al. (2000) have documented an identical chemistry for these two orthogneiss types, and our own field observations suggest that the Gierałtów gneiss is a highly deformed variety of the Sněžník gneiss. Opletal et al. (1980) suggested a pre-Variscan age for the last distinctive tectono-metamorphic imprint to have affected the western part of the OSC, whereas Přikryl et al. (1996) differentiated between an early, pre-Variscan, high-temperature event D_1 that produced E/W-trending ductile fabrics and a later, Variscan, lower temperature overprint D_2 generating N/S-trending brittle–ductile fabrics.

Although deformation in the OSC was more intense than in the Jizera gneisses, the protolith character here is relatively obvious. Don and Opletal (1996) described an intrusive contact of the orthogneisses with metasediments in several roof pendants. Opletal (1997) proposed the following evolutionary history for the orthogneisses and supracrustal rocks of the OSC:

1. The orthogneissic protoliths were emplaced into previously folded and metamorphosed supracrustal rocks of the Młynowiec and Stronie groups, believed to be of Neoproterozoic to middle Cambrian age (Opletal et al. 1980; Don and Opletal 1996); thus, the orthogneiss protoliths intruded near the Cambrian/Ordovician boundary (~500 Ma). Metamorphosed polymetallic deposits, including those of cassiterite, scheelite, and topas, occur around the orthogneiss contacts and indicate that the intrusive event was also accompanied by a thermo-pneumatolitic phase.
2. The granitoid rocks and their host supracrustal suites were subsequently transferred into middle parts of the crust during a transpressional event. The supracrustal assemblage underwent a second metamorphic phase, and the granites became foliated and were modified into the Jizera, Krkonoše and Sněžník orthogneisses. Characteristic Barrovian metamorphic minerals, such as garnet, staurolite, or chloritoid, formed during this event. The garnet found in marginal parts of the orthogneisses is identical in chemical composition to the younger garnet in the metasediments (Opletal et al. 1980). Several lines of reasoning, in particular the fact that the earlier garnet generation in the metasediments is demonstrably older than the intrusion of the gneiss protoliths, indicate that this tectono-metamorphic event was of pre-Variscan age (Opletal et al. 1980; Don et al. 1990). We have now confirmed this by dating of a cross-cutting microgranite dyke at ~492 Ma (sample CS 72; see below).
3. The aforementioned event was followed by uplift of the Jizera, Krkonoše, and Orlické hory blocks, associated with transtension (Cymerman 1997), during which a suite of probably pre-Variscan plutonic rocks was emplaced, ranging from gabbro through tonalite to granite. Some of these intrusions formed contact aureoles in their host rocks. A typical feature of this phase is retrograde metamorphism in the older gneisses, varying in intensity throughout the OSC and producing chloritized garnet and biotite. Lamprophyric dykes dated by K–Ar at 363–390 Ma intruded towards the end of this event, and some of these also formed contact aureoles in the older rocks (Opletal et al. 1980).

Kröner et al. (2000) related the evolution of the granitoid orthogneisses in the OSC to a major Cambro-Ordovician magmatic event in front of a retreating south-dipping subduction zone during progressive closure of the Tornquist ocean southeast of Avalonia, and this scenario is further developed in this paper.

Previous geochronology

Borkowska et al. (1980) dated seven samples of typical Jizera Gneiss by the whole-rock Rb–Sr method and obtained an isochron age of 462±15 Ma, whereas four samples of Jizera leucogneiss yielded an identical age of 473±16 Ma. These data were interpreted to reflect the time of emplacement of the original granite from which the gneisses were derived. More recently, Korytowski et al. (1993) obtained a U–Pb multigrain zircon age of 515+5/–7 Ma for weakly deformed Izera

Gneiss from the eastern bank of Lake Pilkowickie (NW of Jelenia Gora, Poland). An identical multigrain U–Pb zircon age of 514+5/–6 Ma was obtained by Philippe et al. (1995) on Izera metagranite from Perla Zachodu, also in Poland, and the isotopic systematics of these zircons indicated inheritance from ~2430-Ma-old crustal material.

The Sněžník Gneiss and Stronie Formation (Schneeberggneis and Seitenberger Glimmerschiefer in the old German literature) occur in the southeastern Polish Sudetes around the town of Ladek and in the Orlické hory (Fig. 2) on the Czech side of the Orlice-Sněžnik Complex. The various interpretations of the German and Polish schools concerning these rocks were summarized by Borkowska et al. (1990) and Borkowska and Dörr (1998). Van Breemen et al. (1982) dated eight specimens of medium- to coarse-grained granitoid orthogneiss from the OSC at Nová Vieska near Žulová, using the Rb–Sr whole-rock method, and obtained an errorchron age of 487± 11 Ma, whereas Borkowska et al. (1990) dated four large samples of the Sněžník augengneiss using the same method and obtained an isochron age of 395± 35 Ma. Both groups of authors considered these ages to reflect the minimum time of emplacement of the gneiss precursors.

Oliver et al. (1993) were the first to provide U–Pb ages for small multigrain zircon fractions from igneous rocks of the Polish Sudetes, including the Jizera and Orlické-Sněžník complexes, and recognized the complexities of these rocks as documented by their difficult-to-interpret zircon populations, reflecting Pb-loss combined with inheritance. Their sample of Jizera gneiss yielded three strongly discordant zircon fractions indicating Archaean inheritance and possible emplacement of the gneiss protolith sometime between 480 and 504 Ma, whereas three zircon fractions of their Sněžník gneiss suggested crystallization of the gneiss precursor at 504±3 Ma.

Turniak et al. (2000) reported identical single zircon SHRIMP U–Pb ages of 495±7 and 495±14 Ma for two samples of Sněžník and Gierałtow Gneiss, respectively, from the Polish side of the OSC near the village of Midzygórze. They also showed that these zircons contain inherited components as old as 2.6 Ga and determined an imprecise age of 340 Ma for thin overgrowth around some igneous grains that they related to regional high-grade metamorphism in the OSC.

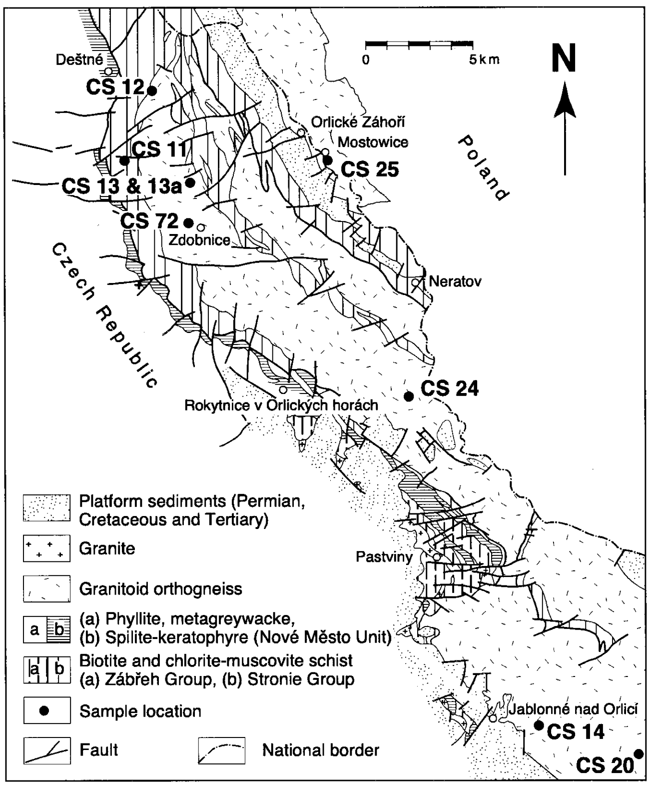

Fig. 2 Simplified geological map of the Orlické hory showing major rock units and sample locations. (Modified after Opletal et al. 1980)

Analytical procedures

Major and trace elements were determined by XRF on fused glass discs and powder pellets, respectively, at the University of Mainz (Germany) using a Philips PW 1404 X-ray fluorescence spectrometer (Laskowski and Kröner 1985). These data are presented in Table 1, together with CIPW normative values for the feldspar phases from which the rock names were derived, using the triangular diagram of O'Connor (1965). Zircons were separated using a Wilfley table, magnetic separator, heavy liquids, and final handpicking. Prior to isotopic analysis, representative zircons of each sample were placed on an epoxy mount and investigated under cathodoluminescence (CL) on a JEOL Superprobe at the University of Mainz. The CL images reveal normal igneous zonation in all cases as is demonstrated for zircons from sample CS 21. Single zircons were analyzed using the evaporation and vapour transfer methods. In addition, we determined the Sm–Nd whole-rock isotopic composition of the dated samples in order to calculate Nd model ages and $\varepsilon_{Nd(t)}$ values.

Vapor transfer technique

The vapor transfer technique (VTT) was first developed by Krogh (1978) and Parrish (1987) and was modified by Wendt and Todt (1991). Our analytical procedures are detailed by Wendt (1993), Jaeckel et al. (1997), and Kröner et al. (1999). Since the zircons are not weighed, no U and Pb concentrations can be calculated, but the use of the mixed spike allows calculation of the ratio of total U over radiogenic Pb. We used a Finnigan-MAT 261 mass spectrometer at

Table 1 Chemical composition of samples dated in this study. Major elements in weight percent, trace elements in parts per million

Sample no.	CS 3	CS 4	CS 5	CS 6	CS 8	CS 9	CS11	CS12	CS13	CS 13A	CS14	CS20	CS21
SiO_2	75.44	76.99	77.30	70.22	75.06	77.95	63.34	76.14	77.44	75.19	71.50	72.05	75.83
TiO_2	0.10	0.07	0.13	0.47	0.10	0.08	0.64	0.12	0.07	0.14	0.33	0.32	0.14
Al_2O_3	13.24	12.68	12.31	14.94	13.57	12.68	15.13	13.01	12.32	13.15	14.92	14.27	12.68
FeO	0.35	0.47	0.92	2.32	1.08	0.84	4.65	0.56	0.72	1.03	1.30	1.49	1.02
Fe_2O_3	0.60	0.83	0.65	0.79	0.62	0.76	1.52	0.93	0.63	0.71	0.99	0.69	0.58
MnO	0.01	0.02	0.03	0.06	0.06	0.03	0.21	0.02	0.03	0.03	0.03	0.03	0.03
MgO	0.16	0.14	0.22	1.00	0.19	0.21	2.27	0.22	0.22	0.26	0.58	0.62	0.20
CaO	0.33	0.25	0.38	0.90	0.40	0.33	3.40	0.25	0.25	0.28	1.26	1.36	0.61
Na_2O	2.94	3.15	2.80	4.39	2.59	3.17	3.64	2.71	3.06	2.86	3.31	3.02	2.68
K_2O	5.11	4.65	4.70	3.62	5.06	2.54	2.36	4.96	4.57	5.02	4.75	4.70	4.90
P_2O_5	0.17	0.20	0.19	0.17	0.25	0.22	0.16	0.17	0.16	0.11	0.20	0.18	0.21
LOI	1.42	1.02	0.84	1.18	1.35	1.29	2.41	1.10	0.88	1.36	1.02	0.70	0.99
Total	**99.88**	**100.47**	**100.47**	**100.06**	**100.33**	**100.10**	**99.73**	**100.19**	**100.35**	**100.14**	**100.19**	**99.43**	**99.87**
Ab	25.27	26.80	23.78	37.57	22.14	27.15	31.84	23.14	26.03	24.50	28.24	25.13	22.93
An	0.53	0.0	0.65	3.39	0.35	0.20	16.35	0.13	0.20	0.68	4.99	5.48	1.67
Or	30.67	27.63	27.88	21.64	30.21	15.19	14.42	29.58	27.15	30.03	28.31	27.31	29.29
Rock type	Granite	Granite	Granite	Granite	Granite	Granite	Grano-diorite	Granite	Granite	Granite	Granite	Granite	Granite
V	<5	–	–	46	–	–	139	13	–	<1	28	26	<8
Cr	10	9	10	23	12	11	38	13	12	10	20	17	8
Co	170	138	161	91	109	107	63	156	146	112	87	134	174
Ni	3	–	–	–	–	–	–	18	–	3	–	0	0
Cu	6	–	2	13	3	–	46	–	4	6	4	5	0
Zn	22	19	42	49	42	28	99	25	37	33	50	36	34
Ga	19	20	19	18	24	24	16	19	18	19	19	17	18
Rb	308	330	311	123	517	252	73	305	325	320	171	183	261
Sr	27	20	25	129	12	50	321	24	25	24	120	103	26
Y	19	15	25	38	23	12	31	19	16	25	43	35	34
Zr	70	63	77	196	72	64	136	79	53	82	154	135	87
Nb	10	9	8	10	13	11	8	7	7	9	11	9	9
Ba	66	–	113	893	74	40	751	98	96	109	735	635	113

The normative minerals Ab, An and Or, calculated from the CIPW norm, were plotted in the triangular diagram of O'Connor (1965) to obtain the rock type

the Max-Planck-Institut für Chemie in Mainz, operated in peak jumping mode and employing a secondary electron multiplier. Blank values were 3 pg for Pb and 10 pg for U. The Pb-composition of the blank was $^{206}Pb/^{204}Pb=17.78$, $^{207}Pb/^{204}Pb=14.97$, $^{208}Pb/^{204}Pb=36.57$. Mass fractionation was 3.5‰ per atomic mass unit for Pb and 2.8‰ for U. Common Pb correction followed the two-stage model of Stacey and Kramers (1975). Regression line calculation was after York (1969), and all errors are given at the 2-σ level. The analytical results are reported in Table 2 and are shown in the Concordia diagrams of Figs. 6, 7 and 8.

Single zircon evaporation

We used the method developed by Kober (1986, 1987), and our laboratory procedures as well as comparisons with conventional and ion-microprobe zircon dating are detailed by Kröner and Todt (1988), Kröner et al. (1991), and Kröner and Hegner (1998). Isotopic measurements were carried out on a Finnigan-MAT 261 mass spectrometer.

The calculated ages and uncertainties are based on the means of all ratios evaluated and their 2-σ mean errors. Mean ages and errors for several zircons from the same sample are presented as weighted means of the entire population. During the course of this study we repeatedly analyzed fragments of large zircon grains from the Palaborwa Carbonatite, South Africa. These magmatic zircons, used as an internal standard, are completely homogeneous when examined under cathodoluminescence. Conventional U–Pb analyses of six separate grain fragments from this sample yielded a $^{207}Pb/^{206}Pb$ age of 2052.2±0.8 Ma (2σ; W. Todt, unpublished data), whereas the mean $^{207}Pb/^{206}Pb$ ratio for 18 grains, evaporated individually over a period of 12 months, is 0.126634±0.000026 (2-σ error of the population), corresponding to an age of 2051.8±0.4 Ma, identical to the U–Pb age. The above error is considered the best estimate for the reproducibility of our evaporation data and approximately corresponds to the 2-σ (mean) error reported for individual analyses in this study (Table 2). In the case of pooled analyses the 2-σ (mean) error may become very low, and whenever this error was less than the reproducibility of the

Table 2 Results of vapor digestion U–Pb isotopic analyses of single zircons or small grain fractions from orthogneisses and metasediments of the Czech West Sudetes

Sample no.	U/Pb[a]	$^{206}Pb/^{204}Pb^{m}$	$^{207}Pb/^{206}Pb^{c}$	$^{206}Pb/^{238}U^{c}$	$^{207}Pb/^{235}U^{c}$	$^{207/206}$ Age	Correlation coefficient
CS 6 P1	14.9	238.7	0.0580±12	0.0602±6	0.482±13	531±46	0.368
CS 6 P1A	3.81	239.4	0.0588±17	0.0730±5	0.592±18	558±62	0.170
CS 6 P2	5.72	819	0.1280±8	0.1530±17	2.700±49	2070±11	0.869
CS 6 P3	13.6	476.8	0.0573±6	0.0664±6	0.524±9	503±22	0.658
CS 6 P3A	13.5	490.4	0.0573±6	0.0668±5	0.528±9	503±21	0.602
CS 6 P4	12.7	388.6	0.0575±9	0.0691±6	0.548±12	510±35	0.466
CS 6 P4A	9.15	515	0.0749±6	0.0944±8	0.975±18	1065±16	0.714
CS 6 P5	7.18	2864	0.1158±6	0.1191±9	1.902±27	1892±10	0.811
CS 6 P5A	12.0	545	0.0575±5	0.0733±4	0.581±12	510±19	0.510
CS 6 P6	12.3	504	0.0590±8	0.0727±9	0.592±18	568±29	0.648
CS 6 P6A	12.4	915	0.0615±8	0.0696±14	0.590±22	656±28	0.822
CS 8 P1	10.9	93.27	0.0600±17	0.0808±6	0.669±35	605±59	0.234
CS 8 P3	12.5	429.5	0.0573±8	0.0701±9	0.554±22	504±32	0.617
CS 8 P5	13.3	379.1	0.0573±4	0.0680±6	0.537±15	503±17	0.728
CS 8 P6	13.4	316.6	0.0573±8	0.0663±9	0.523±20	503±30	0.686
CS 9 P1	13.3	381.1	0.0640±7	0.0689±4	0.608±13	741±22	0.425
CS 9 P2	17.6	803.3	0.0575±3	0.0522±2	0.414±5	511±10	0.622
CS 9 P2A	13.8	7098	0.0647±4	0.0654±5	0.583±12	764±13	0.785
CS 9 P3	13.5	2188	0.0573±4	0.0666±7	0.527±10	506±14	0.846
CS 9 P3A	13.5	4441	0.0597±3	0.0679±5	0.559±8	594±12	0.779
CS 9 P4A	11.3	1005	0.0575±3	0.0813±6	0.644±10	510±11	0.813
CS 9 P5	15.7	1533	0.0587±5	0.0587±7	0.475±11	555±17	0.816
CS 9 P6	16.1	1124	0.0575±2	0.0571±3	0.453±6	509±9	0.826
CS 11 P1	3.80	1759	0.1189±4	0.2154±13	3.530±43	1939±5	0.893
CS 11 P2	8.81	723	0.0620±7	0.0884±16	0.756±30	674±23	0.855
CS 11 P3	9.36	357	0.0589±11	0.0896±7	0.728±24	564±40	0.362
CS 11 P4	6.49	1520	0.0818±3	0.1267±10	1.428±23	1240±8	0.889
CS 11 P5	9.63	678	0.0615±5	0.0803±6	0.680±18	656±18	0.635
CS 13A P1	12.3	2044	0.0646±5	0.0730±6	0.650±13	762±17	0.664
CS 13A P2	15.6	876	0.0572±16	0.0576±8	0.454±20	500±60	0.431
CS 13A P5	19.0	269.8	0.0573±8	0.0457±5	0.361±22	504±32	0.560
CS 13A P6	18.4	744	0.0575±14	0.0493±11	0.391±18	511±54	0.633
CS 14 P4	15.5	507	0.0574±17	0.0583±39	0.462±46	508±65	0.909
CS 14 P5	13.0	368.6	0.0574±16	0.0698±7	0.553±21	506±62	0.461
CS 14 P6	15.5	473.4	0.0573±7	0.0595±4	0.470±11	505±25	0.228
CS 18 P2	12.4	370.1	0.0662±18	0.0712±7	0.650±24	813±55	0.301
CS 18 P3	9.84	8387	0.1183±8	0.0767±8	1.252±24	1931±12	0.818
CS 18 P4	13.9	220.6	0.0676±23	0.0635±8	0.591±28	855±72	0.294
CS 18 P5	12.6	166.5	0.0647±19	0.0701±7	0.625±21	766±62	0.301
CS 20 P1A	13.7	1151	0.0589±4	0.0670±6	0.545±14	564±15	0.773
CS 20 P2A	16.3	2521	0.0666±4	0.0562±6	0.516±10	826±11	0.894
CS 20 P6A	26.3	1479	0.0573±4	0.0342±4	0.270±6	503±15	0.824
CS 21 P1	14.2	1003	0.0575±4	0.0646±4	0.512±7	512±15	0.662
CS 21 P2	13.9	737	0.0575±3	0.0663±5	0.526±7	511±11	0.796
CS 21 P3	12.9	1281	0.0575±4	0.0718±6	0.570±10	511±15	0.778
CS 21 P4	16.1	987	0.0575±10	0.0575±5	0.456±10	511±36	0.740
CS 21 P5	14.0	1678	0.0575±3	0.0663±5	0.526±8	511±11	0.800
CS 24 P1	13.1	307.9	0.0652±7	0.0671±6	0.603±15	782±23	0.587
CS 24 P1B	8.96	2029	0.0842±4	0.0982±5	1.140±14	1298±10	0.723
CS 24 P2	14.2	286.3	0.0574±6	0.0624±5	0.494±13	508±25	0.594
CS 24 P2B	17.2	203.1	0.0574±23	0.0515±4	0.407±17	506±86	0.137
CS 24 P3	15.4	182.3	0.0575±13	0.0575±3	0.456±11	512±50	0.194
CS 24 P5/6	13.3	373.1	0.0575±4	0.0685±6	0.543±11	510±13	0.787
CS 25 P1	15.6	310.9	0.0574±17	0.0588±7	0.466±22	509±63	0.587
CS 25 P1A	13.7	505	0.0575±6	0.0652±5	0.517±15	511±25	0.546
CS 25 P2	14.2	305.9	0.0614±19	0.0627±10	0.531±30	653±66	0.432
CS 25 P2A	16.0	285.8	0.0614±13	0.0563±4	0.477±17	655±46	0.256
CS 25 P2B	16.3	251.7	0.0588±7	0.0536±4	0.434±17	559±27	0.449
CS 25 P3B	14.7	349.6	0.0575±7	0.0618±4	0.490±17	510±28	0.440
CS 25 P4	17.6	196.3	0.0725±14	0.0486±3	0.485±10	999±38	0.263
CS 25 P5	15.1	309.9	0.0636±20	0.0580±7	0.508±48	727±67	0.333
CS 25 P5A	13.3	461.3	0.0575±8	0.0669±17	0.530±35	510±30	0.881
CS 25 P5B	17.8	266.8	0.0585±13	0.0508±5	0.410±17	549±47	0.378

[a] Small grain fractions

internal standard we used the latter value, i.e., an assumed 2-σ_m error of 0.000026.

The analytical data are presented in Table 3, and the $^{207}Pb/^{206}Pb$ spectra are shown in histograms that permit visual assessment of the data distribution from which the ages are derived. The evaporation technique only provides Pb isotopic ratios, and there is no a priori way to determine whether a measured $^{207}Pb/^{206}Pb$ ratio reflects a concordant age. Thus, principally, all $^{207}Pb/^{206}Pb$ ages determined by this method are necessarily minimum ages. However, many studies have demonstrated that there is a very strong likelihood of these data to represent true zircon crystallization ages (a) when the $^{207}Pb/^{206}Pb$ ratio does not change with increasing temperature of evaporation, and/or (b) when repeated analysis of grains from the same sample at high evaporation temperatures yield the same isotopic ratios within error. Comparative studies by single grain evaporation, conventional U–Pb dating, and ion-microprobe analysis have shown this to be correct (e.g., Kröner et al. 1991; Cocherie et al. 1992; Jaeckel et al. 1997; Karabinos 1997; Kröner et al. 1999).

Sm–Nd analysis

Sm–Nd isotopic analyses were carried out in the radiogenic isotope laboratory of the University of Tübingen using a technique described by Hegner et al. (1995) and Kröner and Hegner (1998). Total procedural blanks were <30 pg for Nd and Sm, and are not significant for the samples under investigation.

Isotopic ratios were measured in dynamic quadruple collector using a MAT 262 mass spectrometer. $^{143}Nd/^{144}Nd$ ratios are normalised to $^{146}Nd/^{144}Nd=0.7219$, and Sm isotopic ratios to $^{147}Sm/^{152}Sm=0.56081$. During the course of this study the La Jolla Nd standard yielded $^{143}Nd/^{144}Nd=0.511849\pm5$ (2σ, n=16). Within-run precision (2-σ mean) for Nd is 10^{-5}. The error in the $^{147}Sm/^{144}Nd$ ratio is ~0.2%.

The Nd isotopic data are summarized in Table 4. The $\varepsilon_{Nd(t)}$ values were calculated for the zircon age determined for each sample. The Nd model ages are based on the parameters of Liew and Hofman (1988). Due to the low Sm/Nd ratios in most samples, initial ε_{Nd} values are not significantly affected by age uncertainties up to 20 Ma. We interpret the Nd model ages in terms of mean crustal residence ages (Arndt and Goldstein 1987).

Petrography, geochemistry, and zircon geochronology

We report our results from NW to SE, beginning with the Jizerské hory and Krkonoše Mountains and then moving to the Orlické hory and the Orlice-Sněžník Complex (OSC).

Jizerské hory

Samples CS 3–5 represent medium- to coarse-grained augengneisses derived from porphyritic granites, also known as Rumburk Granite (Domečka 1970), and are exposed near the small town of Frýdlant (Fig. 1). These rocks extend into Poland where they are known as Izera Gneiss (Kozłowska-Koch 1965; Żaba 1984). The above samples are all similar in chemical composition and correspond to granite (Table 1). All three samples contain abundant near-idiomorphic, long-prismatic zircons with slight rounding at their terminations which was caused by "metamorphic corrosion" (see Fig. 3a; Gastil et al. 1967; Silver 1969; Kröner et al. 1994a, 1994b). This occurs during upper amphibolite and granulite facies metamorphism when dissolution of zircon and subsequent "healing" through recrystallization begin preferentially at prism ends.

Several of these zircon grains were analyzed from sample CS 3 of which three yielded almost identical $^{207}Pb/^{206}Pb$ ratios that produced a combined mean age of 504.6±1.2 Ma (Fig. 4a; Table 2). In view of the consistency of this result with those from other samples reported herein we interpret this age to approximate the time of igneous emplacement of the original granite from which the present gneiss was derived. Two additional grains with slightly more pronounced rounding than those reported above produced substantially higher $^{207}Pb/^{206}Pb$ ratios with ages of 846.2±2.6 and 1706.8±2.2 Ma, respectively (Table 3, Fig. 4b,c). These grains were either inherited from the source region from where the precursor granite of sample CS 3 was ultimately derived by intracrustal melting, or they represent true xenocrysts captured from the wall rock during ascent of the granite magma. We were unable to distinguish between these two alternatives

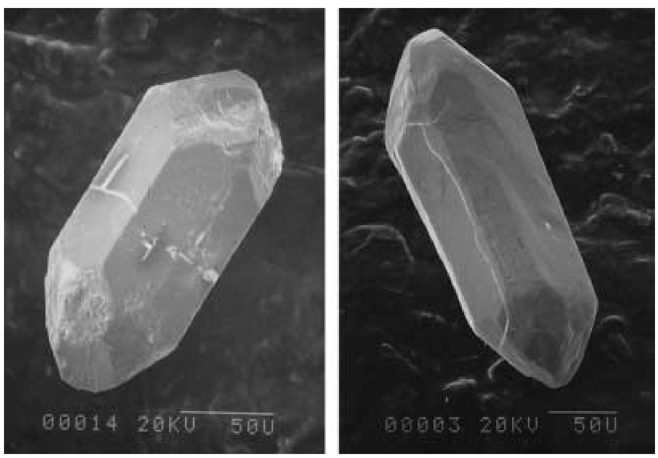

Fig. 3a,b Scanning electron microscope photographs showing zircon morphologies from orthogneisses of the Krkonoše Mountains and Orlické hory, Czech West Sudetes. **a** Zircon from sample CS 6 showing damage on pyramidal crystal planes due to metamorphic "corrosion". **b** Zircon from sample CS 24 showing well-recrystallized pyramidal terminations with development of new facets

Table 3 Sm–Nd isotopic systematics for granitoid orthogneisses of the Czech West Sudetes

Sample no.	Zircon colour and morphology	Grain no.	Mass scans[a]	Evaporation temperature (in °C)	Mean ^{207}/Pb/^{206}Pb ratio and 2-σ_m error[b]	^{207}Pb/^{206}Pb age and 2-σ_m error
CS 3	Clear to yellow, long-prismatic, idiomorphic	1	84	1596	0.057323±56	504.0±2.2
		2	54	1599	0.057358±75	505.3±2.9
		3	85	1602	0.057340±30	504.6±1.1
Mean of 3		1–3	204		0.057338±32	**504.6±1.2**
	Yellow, ends rounded pink, ends rounded	4	61	1599	0.067273±85	846.2±2.6
		5	44	1600	0.104574±127	1706.8±2.2
CS 4	Clear, long-prismatic, idiomorphic	1	102	1608	0.057392±49	506.6±1.9
		2	115	1601	0.057378±41	506.1±1.6
		3	73	1602	0.057359±52	505.4±2.0
		4	62	1599	0.057369±64	505.8±2.4
Mean of 4		1–4			0.057376±25	**506.0±1.0**
	Pink, long-prismatic, idiomorphic	5	62	1599	0.066640±53	826.6±1.6
		6	40	1596	0.066796±98	831.4±3.0
Mean of 2		5, 6	102		0.066702±52	**828.5±1.6**
	Clear, long-prismatic, slightly rounded ends	7	118	1601	0.067124±42	841.6±1.3
		8	98	1600	0.067124±41	841.6±1.3
Mean of 2		7, 8	216		0.067124±30	**841.6±0.9**
	Clear, long-prismatic, slightly rounded ends	9	44	1608	0.067624±88	857.1±2.7
		10	63	1597	0.067751±45	860.9±1.4
Mean of 2		9, 10	107		0.067698±46	**859.3±1.4**
	Clear, rounded ends	11	39	1598	0.069565±75	915.5±2.2
CS 5	Clear to light brown, long-prismatic, idiomorphic	1	104	1601	0.057580±34	513.8±1.3
		2	109	1607	0.057606±34	514.8±1.3
		3	63	1606	0.057617±67	515.2±2.6
Mean of 3		1–3			0.057599±24	**514.5±1.0**[c]
	Yellow-brown stubby brown, idiomorphic, stubby yellow-brown stubby yellow-brown stubby pink, long, idiomorphic stubby, ends rounded	4	95	1598	0.058437±47	546.2±1.8
		5	31	1600	0.061087±153	642.3±5.4
		6	62	1606	0.061641±83	661.7±2.9
		7	28	1597	0.063600±121	728.3±4.0
		8	65	1596	0.066291±78	815.6±2.5
		9	39	1594	0.076384±73	1105.2±1.9
CS 6	Clear to pink, long-prismatic, idiomorphic	1	76	1602	0.057175±79	498.3±3.0
		2	90	1598	0.057269±41	501.9±1.6
		3	85	1603	0.057280±60	502.3±2.3
		4	64	1597	0.057292±62	502.8±2.4
		5	75	1598	0.057279±79	502.3±3.0
Mean of 5		1–5	390		0.057259±29	**501.5±1.1**
	Yellow-brown stubby clear, stubby, ends slightly rounded as above	6	31	1607	0.066228±126	813.6±4.0
		7	62	1596	0.073963±68	1040.5±1.9
		8	53	1601	0.082607±157	1259.9±2.7
		9	30	1609	0.112954±165	1847.5±2.6
CS 8	Clear to pink, long-prismatic, idiomorphic	1	86	1604	0.057318±31	503.8±1.2
		2	82	1602	0.057310±36	503.5±1.4
		3	86	1609	0.057287±34	502.6±1.3
		4	84	1598	0.057296±32	503.0±1.2
Mean of 4		1–4	338		0.057303±16	**503.2±1.0**[c]
	Yellow-brown, stubby to long-prismatic, idiomorphic	5	54	1602	0.058168±93	536.1±3.5
		6	84		0.058169±70	536.1±2.6
		7	84	1600	0.058171±76	536.2±2.8
		8	65	1600	0.058173±51	536.2±1.9
Mean of 4		5–8	287		0.058170±36	**536.2±1.4**
	Pink to yellow-brown, stubby to long-prismatic, ends very slightly rounded	9	65	1602	0.058472±51	547.5±1.9
		10	63	1599	0.059109±74	571.1±2.7
		11	105	1598	0.062271±33	683.4±1.1
		12	147	1602	0.062651±38	696.4±1.3
		13	102	1601	0.068445±55	882.1±1.7
CS 9	Clear to yellow-brown, long-prismatic, idiomorphic	1	87	1606	0.057536±48	512.1±1.8
		2	59	1598	0.057495±40	510.6±1.5
		3	64	1596	0.057501±51	510.8±2.0
		4	75	1597	0.057498±46	510.7±1.8
Mean of 4		1–4	285		0.057510±24	**511.1±1.0**[c]

Table 3 Continued

Sample no.	Zircon colour and morphology	Grain no.	Mass scans[a]	Evaporation temperature (in °C)	Mean ^{207}Pb/^{206}Pb ratio and 2-σ_m error[b]	^{207}Pb/^{206}Pb age and 2-σ_m error
CS 11	Short-prismatic, grey long-prismatic, euhedral	1	42	1595	0.067138±54	842.1±1.7
		2	77	1597	0.093458±77	1497.2±1.6
CS 12	Clear, long-prismatic, idiomorphic	1	74	1596	0.057397±79	506.8±3.0
		2	74	1597	0.057400±65	506.9±2.5
		3	106	1600	0.057411±38	507.3±1.4
Mean of 3		1–3	254		0.057404±33	**507.1±1.3**
	Stubby, ends rounded	4	41	1592	0.074915±120	1066.2±3.2
CS 13	Yellow-brown to grey-brown, stubby, idiomorphic	1	65	1598	0.057284±53	502.5±2.1
		2	131	1598	0.057328±46	504.2±1.7
		3	95	1601	0.057301±44	503.3±1.7
Mean of 3		1–3	291		0.057310±28	**503.5±1.1**
	Yellow-brown, ends rounded, stubby	4	68	1600	0.060262±61	613.0±2.2
		5	44	1599	0.065135±82	778.7±2.7
CS 13a	Yellow-brown to grey-brown, long-prismatic, idiomorphic	1	73	1602	0.057273±74	502.1±2.8
		5	85	1600	0.057299±50	503.1±1.9
		6	52	1600	0.057301±52	503.2±2.0
Mean of 3		1–3	210		0.057294±32	**502.9±1.2**
Mean of 6 (CS 13+CS 13a)		6	501		0.057303±21	**503.2±1.0**[c]
CS 14	Clear to yellowish, long-prismatic, idiomorphic	1	76	1598	0.057339±45	504.6±1.7
		2	66	1599	0.057318±46	503.8±1.8
		3	88	1596	0.057355±39	505.2±1.5
Mean of 3		1–3	230		0.057339±25	**504.6±1.0**[c]
CS 20	Clear, long-prismatic idiomorphic	1	101	1600	0.057299±35	503.1±1.3
		2	95	1598	0.057308±33	503.4±1.3
		3	119	1598	0.057315±30	503.7±1.2
		4	65	1599	0.057282±44	502.4±1.7
		5	39	1603	0.057302±50	503.2±1.9
Mean of 5		1–5	419		0.057303±16	503.2±1.0[c]
	Yellowish-brown ends slightly rounded	6	63	1604	0.062521±73	692.0±2.5
		7	97	1599	0.067957±35	867.2±1.1
		8	85	1596	0.079491±62	1184.4±1.5
CS 2	Clear to yellowish, long-prismatic, idiomorphic	1	73	1598	0.057497±73	510.7±2.8
		2	44	1599	0.057485±61	510.2±2.3
		3	73	1596	0.057514±39	511.3±1.5
Mean of 3		1–3	190		0.057501±34	**510.8±1.3**
CS 24	Clear to light red long-prismatic, idiomorphic	1	59	1596	0.057479±102	510.0±3.9
		2	106	1595	0.057455±60	509.0±2.3
		3	63	1597	0.057486±71	510.2±2.7
		4	75	1596	0.057505±41	511.0±1.6
Mean of 4		1–4	303		0.057478±34	**509.9±1.3**
	Clear, ends rounded	5	66	1596	0.087542±55	1372.5±1.2
CS 25	Clear, long-prismatic idiomorphic	1	41	1597	0.057496±87	510.6±3.3
		2	108	1599	0.057515±36	511.3±1.4
		3	73	1602	0.057457±48	509.1±1.8
Mean of 3		1–3	222		0.057501±34	**510.5±1.1**
CS 72	Clear to pale yellow, stubby to long-prismatic, idiomorphic	1	108	1598	0.056990±18	491.1±0.7
		2	147	1599	0.056996±26	491.6±1.0
		3	104	1600	0.057016±23	492.2±0.9
		4	128	1598	0.057025±18	492.5±0.7
		5	82	1599	0.056986±26	491.0±1.0
		6	110	1597	0.057011±22	492.0±0.9
Mean of 6		1–6	679		0.057005±11	**491.7±1.0**[c]

[a] Number of ^{207}Pb/^{206}Pb ratios evaluated for age assessment
[b] Observed mean ratio corrected for non-radiogenic Pb where necessary. Errors based on uncertainties in counting statistics
[c] Error based on reproducibility of internal standard

Table 4 Sm–Nd isotopic systematics for granitoid orthogneisses of the Czech West Sudetes

Sample	Age (Ma)	Sm (ppm)	Nd (ppm)	$^{147}Sm/^{144}Nd$	$^{143}Nd/^{144}Nd$	$\varepsilon_{Nd(t)}$	T_{DM} (Ga)
CS 3	505	1.44	5.010	0.1734	0.512290	–5.3	1.6
CS 4	506	2.23	9.250	0.1458	0.512290	–5.0	1.5
CS 5	515	5.06	27.02	0.1132	0.512151	–4.2	1.5
CS 6	502	8.58	42.81	0.1211	0.512151	–4.7	1.5
CS 7	(500)	4.45	22.82	0.1179	0.512125	–5.0	1.6
CS 8	503	2.38	8.229	0.1751	0.512307	–5.1	1.6
CS 9	511	1.72	5.747	0.1808	0.512379	–4.0	1.5
CS 11	(520)	5.35	24.59	0.1316	0.512239	–3.5	1.5
CS 12	507	1.83	6.084	0.1814	0.512256	–6.5	1.7
CS 14	505	5.23	22.44	0.1407	0.512137	–6.2	1.7
CS 20	503	5.39	24.16	0.1348	0.512188	–4.8	1.6
CS 21	511	4.96	21.03	0.1426	0.512260	–3.9	1.5
CS 25	511	3.22	11.56	0.1685	0.512337	–4.1	1.5

Rock formation ages based on zircon analyses; ages in parentheses are estimated
$^{143}Nd/^{144}Nd$ 2 σ_m within-run error ~10^{-5}, external precision ~1.5×10^{-5}. Sm and Nd concentrations were determined by isotope dilution, error in $^{147}Sm/^{144}Nd$ ~0.2%. Two-stage T_{DM} model ages based on a depleted mantle evolution curve according to Liew and Hofmann (1988): $^{143}Nd/^{144}Nd$ MORB=0.513151, $^{147}Sm/^{144}Nd$ MORB=0.219, $^{147}Sm/^{144}Nd$ continental crust=0.12

in this and the following samples, but the important conclusion is that there is older Precambrian crust beneath the Jizerské hory. Oliver et al. (1993), Kröner and Hegner (1998), and Kröner et al. (1994a) also reported Precambrian zircon xenocrysts from granitoid gneisses of the Sudetes Mountains and Lusatia, respectively. Since the xenocryst results are, in fact, $^{207}Pb/^{206}Pb$ ages for one zircon grain only, we are unable to verify their accuracy by more measurements, and caution should therefore be exercised to consider them as precise ages as their statistical error would imply. In any case, they are minimum ages and as such provide useful information on the crust below the Sudetes Mountains

The $\varepsilon_{Nd(t)}$ value for whole-rock sample CS 3 for an emplacement age of ~505 Ma is –5.3, and a mean crustal residence age of 1.6 Ga can be calculated (Table 4). The negative $\varepsilon_{Nd(t)}$ value suggests involvement of old crustal material in the generation of the gneiss protolith, as also indicated by the zircon xenocrysts.

Sample CS 4 yielded similar results in that four igneous grains combine to a mean age of 506.0±1.0 Ma (Fig. 4d; Table 3) that we also consider to reflect the time of emplacement of the gneiss precursor. Eleven additional grains produced xenocryst ages, and in several cases these ages could be reproduced from two grains each; these are 828.5±1.6, 841.6±0.9, 859.3±1.4, and 915.5±2.2 Ma, respectively (Fig. 4e–h; Table 3). The $\varepsilon_{Nd(t)}$ value for whole-rock sample CS 4 is –5.0, and the mean crustal residence age, based on a depleted mantle (DM) model, is 1.5 Ga (Table 4). As in the case of CS 3, the negative $\varepsilon_{Nd(t)}$ value suggests involvement of old crustal material in the generation of the original granite, and this interpretation is supported by the zircon xenocrysts.

Sample CS 5 is a strongly foliated granite-gneiss of G'-type (Chaloupský 1989), collected north of the village of Nové Město p.S. (Fig. 1). The zircons are morphologically similar to those in the previous samples, and Fig. 2b shows a grain with severe damage due to metamorphic corrosion but without recrystallization. The three youngest grains analyzed by evaporation have identical $^{207}Pb/^{206}Pb$ ratios that yield a mean age of 514.5±1.0 Ma (Fig. 5a; Table 3), and we interpret this to reflect the time of emplacement of the precursor granite. Numerous additional zircons with similar morphologies to those of the above grains produced significantly higher $^{207}Pb/^{206}Pb$ ratios which correspond to ages of 546.2±1.8, 642.3±5.4, 661.7±2.9, 728.3±4.0, 815.6±2.5, and 1105.2±1.9 Ma, respectively (Fig. 5b–g; Table 2). This large number of xenocrystic zircons attests to the S-type nature of the host granite-gneiss and to a very heterogeneous source from which the gneiss protolith was derived.

The $\varepsilon_{Nd(t)}$ value for whole-rock sample CS 5 is –4.2, and the mean crustal residence age is 1.5 Ga (Table 4). As in the case of the previous samples, the negative $\varepsilon_{Nd(t)}$ value suggests that old crust was involved in the generation of the gneiss protolith, and the numerous zircon xenocrysts support this view.

Krkonoše Mountains

Sample CS 6 is a strongly foliated, almost mylonitic, augengneiss with typical granitic chemistry (Table 1), collected at Špindlerów Mlýn just north of Bedřichov (Fig. 1). The zircons are again similar to those in the previous samples, and 11 grains were analyzed by VTT (Table 2). Four analyses are between 10 and 15% discordant and can be fitted to a chord through the origin intersecting Concordia at 505±17 Ma (Fig. 6a). The remaining analyses are all considerably discordant and have $^{207}Pb/^{206}Pb$ minimum ages ranging from 531 to 2070 Ma (Table 2; not shown in Fig. 6a). Since these grains were not abraded, it is possible that they contained inherited cores and newly formed rims, and some of the resulting isotopic results may there-

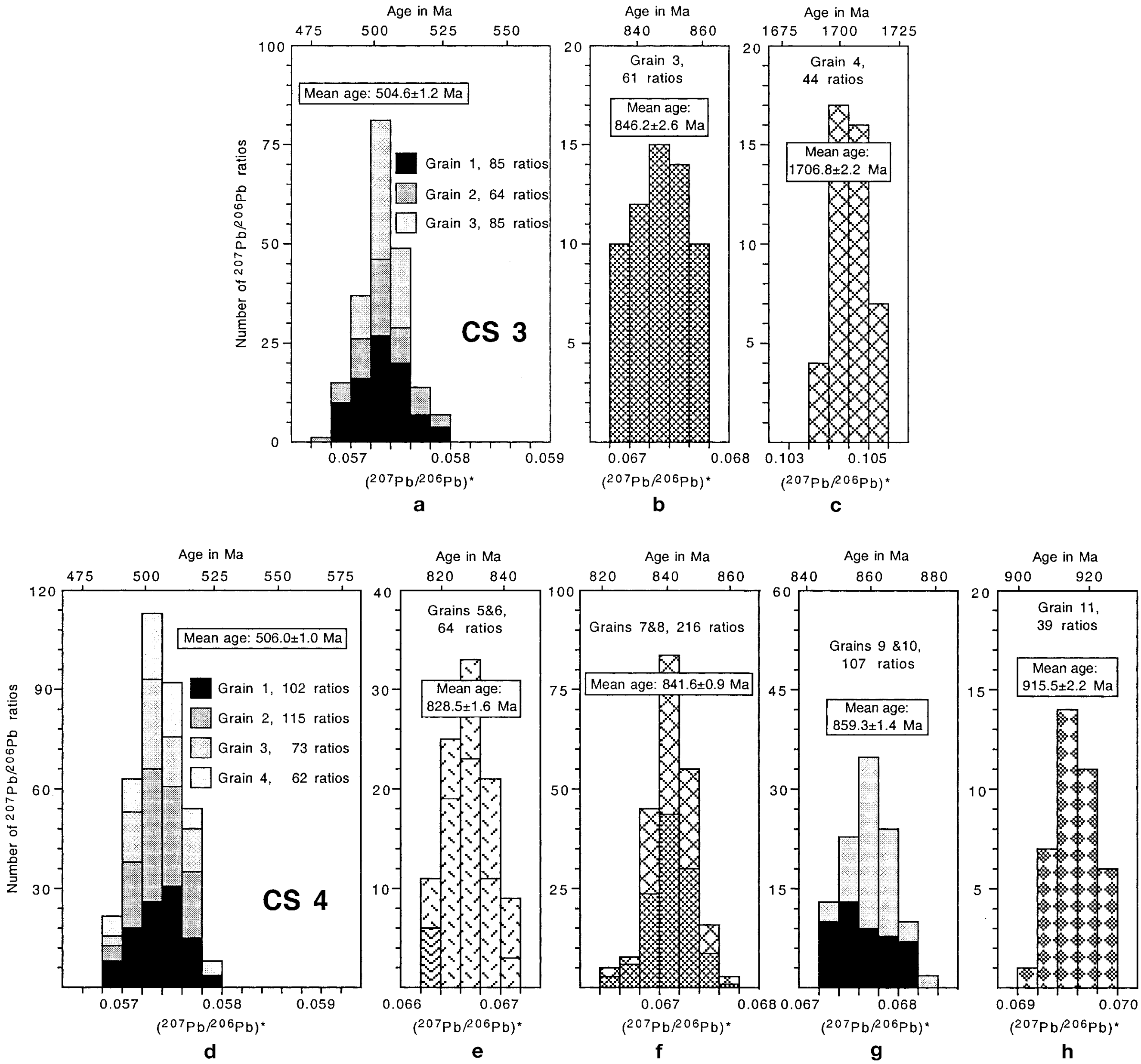

Fig. 4a–h Histograms showing distribution of radiogenic lead isotope ratios derived from evaporation of single zircons from strongly foliated granitoid orthogneiss (augengneiss) samples, Frýdlant, Czech Republic. **a** Spectrum for three grains from porphyritic gneiss sample CS 3, interpreted to reflect age of protolith emplacement. **b–c** Spectra for xenocrystic grains. **d** Spectrum for four grains from pink gneiss sample CS 4, interpreted to reflect age of protolith emplacement. **e–h** Spectra for xenocrystic grains

fore be mixed ages with no direct geological meaning. In any case, we interpret these old grains as xenocrysts, as in the previous cases. In addition, a total of nine zircons was analysed by evaporation, and five grains yielded identical results, combining to a mean $^{207}Pb/^{206}Pb$ age of 501.5±1.1 Ma (Fig. 6a, inset; Table 3). This age is the same, but more precise, than the VTT age, and we interpret this as reflecting the time of emplacement of the gneiss precursor.

Four additional grains produced $^{207}Pb/^{206}Pb$ ages ranging from 814 to 1848 Ma (Table 3; not shown in Fig. 6a), and in view of the fact that these data were

Fig. 5a–k Histograms showing distribution of radiogenic lead isotope ratios derived from evaporation of single zircons from strongly foliated granite gneisses, Jizerské hory, Krkonoše Mountains and Orlické hory, Czech Republic. **a** Spectrum for three grains from sample CS 5 (cataclastic two-mica granite-gneiss, γG-type of Chaloupský 1989), interpreted to reflect age of protolith emplacement. **b–g** Spectra for xenocrystic grains. **h** Spectrum for three grains from sample CS 12 (two-mica granite-gneiss, G-type of Opletal and Domečka 1983), interpreted to reflect age of protolith emplacement. **i** Spectrum for xenocrystic grain. **j** Spectrum for three grains from augengneiss sample CS 13. **k** Spectrum for xenocrystic grain

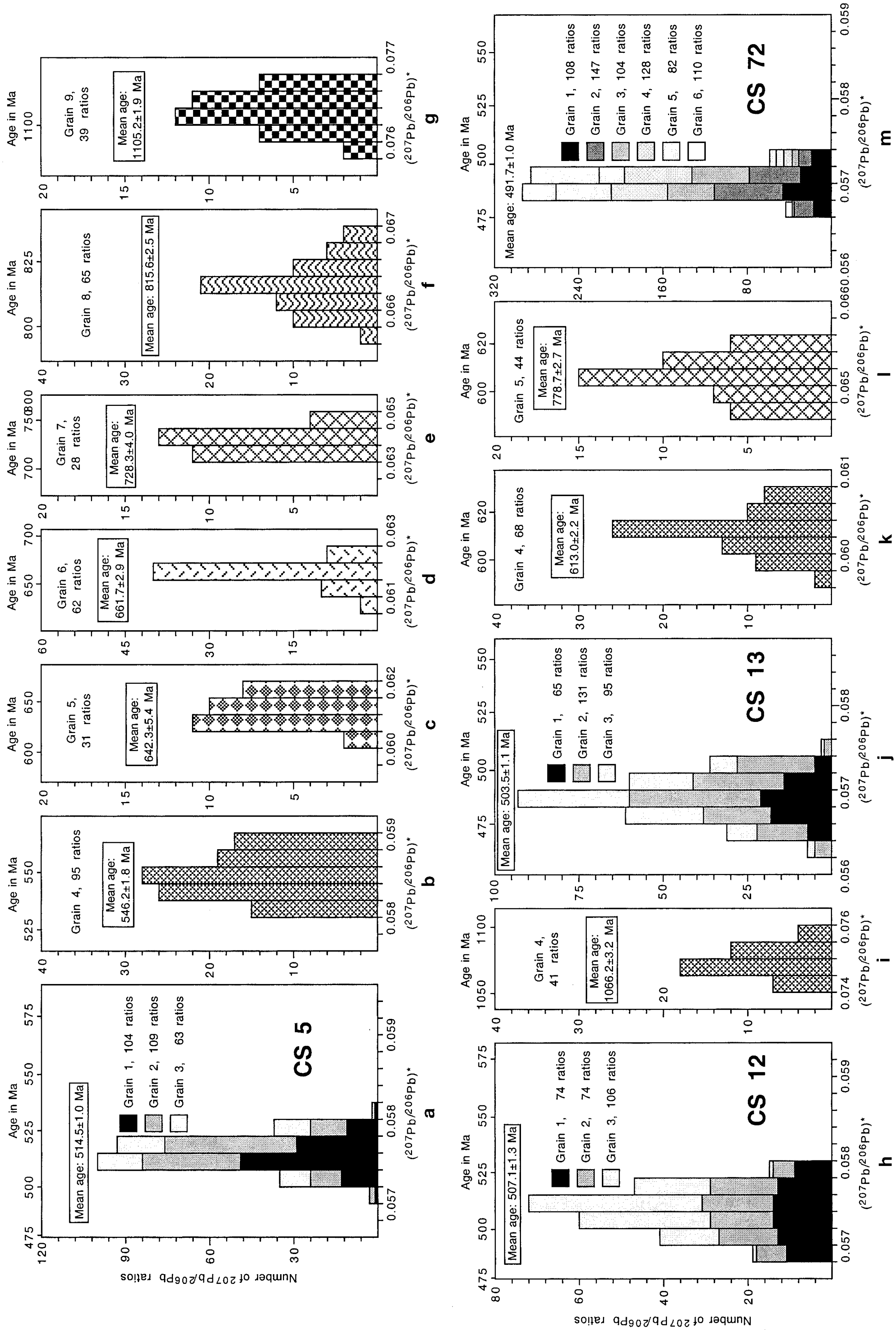

Number of 207Pb/206Pb ratios
Age in Ma
(207Pb/206Pb)*
a
Mean age: 514.5±1.0 Ma
Grain 1, 104 ratios
Grain 2, 109 ratios
Grain 3, 63 ratios
CS 5
b
Grain 4, 95 ratios
Mean age: 546.2±1.8 Ma
c
Grain 5, 31 ratios
Mean age: 642.3±5.4 Ma
d
Grain 6, 62 ratios
Mean age: 661.7±2.9 Ma
e
Grain 7, 28 ratios
Mean age: 728.3±4.0 Ma
f
Grain 8, 65 ratios
Mean age: 815.6±2.5 Ma
g
Grain 9, 39 ratios
Mean age: 1105.2±1.9 Ma
h
Mean age: 507.1±1.3 Ma
Grain 1, 74 ratios
Grain 2, 74 ratios
Grain 3, 106 ratios
CS 12
i
Grain 4, 41 ratios
Mean age: 1066.2±3.2 Ma
j
Mean age: 503.5±1.1 Ma
Grain 1, 65 ratios
Grain 2, 131 ratios
Grain 3, 95 ratios
CS 13
k
Grain 4, 68 ratios
Mean age: 613.0±2.2 Ma
l
Grain 5, 44 ratios
Mean age: 778.7±2.7 Ma
m
Mean age: 491.7±1.0 Ma
Grain 1, 108 ratios
Grain 2, 147 ratios
Grain 3, 104 ratios
Grain 4, 128 ratios
Grain 5, 82 ratios
Grain 6, 110 ratios
CS 72

obtained after several deposition-ionization cycles and high-temperature heating, we are fairly confident that they represent true xenocryst ages, although mixing cannot be completely ruled out. The xenocryst ages produced by both VTT and evaporation attest to the crustal origin of the gneiss precursor and, as in the cases of CS 4 and 5, reveal a heterogeneous late to middle Precambrian basement underneath the Krkonoše Mountains

The $\varepsilon_{Nd(t)}$ value for whole-rock sample CS 6 is –4.7, and the mean crustal residence age is 1.5 Ga (Table 4). The same interpretation as for the previous samples is given, namely that the gneiss precursor was generated predominantly from old crust; however, since the Nd model age is markedly younger than the oldest zircon xenocryst age, this may also mean that some juvenile material was involved, and that the Nd model age reflects mixtures, of unknown proportions, of old and juvenile crust.

Sample CS 8 is also a strongly foliated, almost mylonitic, augengneiss with granitic chemistry (Table 1), collected north of Vrchlabí (Fig. 1). The zircons, as in the previous cases, are clear, pink, and yellow-brown, and long prismatic with very slight rounding at their terminations. Four grains were analyzed by VTT of which three produced consistent, 10–15% discordant, results which can be fitted to a discordia line through the origin intersecting Concordia at 503±35 Ma (Table 2, Fig. 6b). One grain is considerably older at 605±59 Ma (Table 2) and is interpreted as a xenocryst. Thirteen grains were evaporated individually, and the results are shown in Table 3. The four youngest grains produced identical $^{207}Pb/^{206}Pb$ ratios that combine to a mean age of 503.2±1.0 Ma (Fig. 6b, inset). Four additional grains also yielded consistent results with a mean age of 536.2±1.4 Ma (not shown in Fig. 6b). The remaining

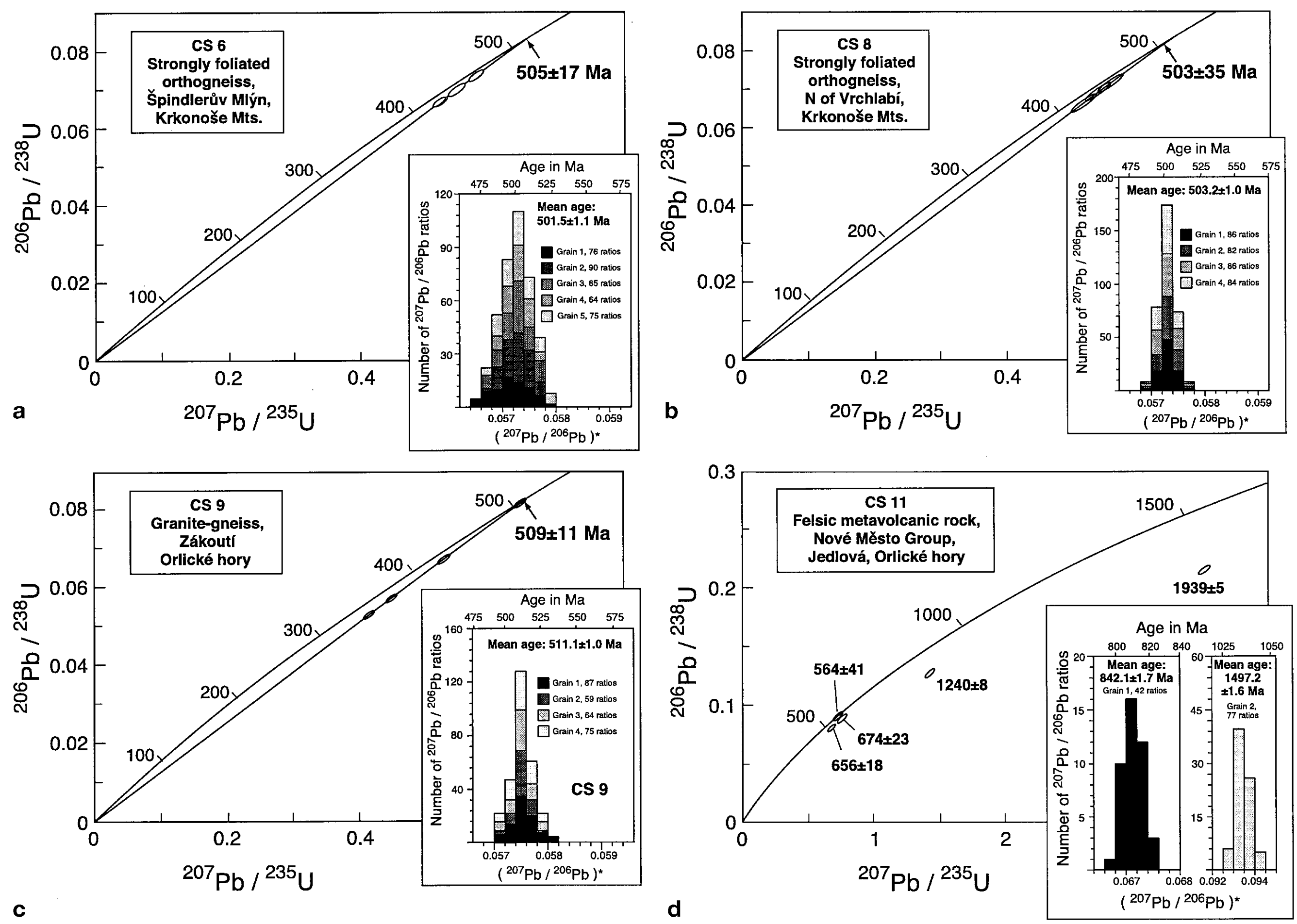

Fig. 6a–d Concordia diagrams and histograms showing analytical data for single zircons from granitic gneiss samples of the Krkonoše Mountains and Orlické hory, Czech West Sudetes. **a** Four grains from strongly foliated augengneiss sample CS 6. *Inset* shows histogram with distribution of radiogenic lead isotope ratios derived from evaporation of five single zircons from same sample. **b** Three grains from strongly foliated granite-gneiss sample CS 8. *Inset* shows histogram with distribution of radiogenic lead isotope ratios derived from evaporation of four single zircons from same sample. **c** Three grains from granite-gneiss sample CS 9. *Inset* shows histogram with distribution of radiogenic lead isotope ratios derived from evaporation of four single zircons from same sample. **d** Five grains from felsic tuff sample CS 11. *Inset* shows histogram with distribution of radiogenic lead isotope ratios derived from evaporation of two single zircons from same sample

five analyses vary between 548 and 882 Ma (not shown in Fig. 6b). In view of the excellent agreement between the VTT and evaporation analyses, we interpret the age of ~503 Ma as approximating the time of intrusion of the granitic gneiss precursor, all the more so since this age is also very similar to the emplacement ages calculated for the previous samples. The age of 536 Ma probably reflects a major late Neoproterozoic crustal component in the source region of the original granite since it is well represented in the xenocrystic zircon population of sample CS 8. Rocks of this age occur in the neighboring terrains of Lusatia (Kröner et al. 1994a) and the Erzgebirge Mountains (Kröner et al. 1995), and are likely to be present below the Krkonoše Mountains The older xenocryst ages are consistent with the results for samples CS 3–6.

The $\varepsilon_{Nd(t)}$ value for whole-rock sample CS 8 is –5.1, and a mean crustal residence age of 1.6 Ga can be calculated (Table 4). As for the previous samples, the gneiss precursor was generated predominantly from old crust.

Orlice-Śněžník Complex (OSC)

Sample CS 9 represents a grey to pinkish, well-foliated, fine-grained granite-gneiss of G-type (Opletal et al. 1980) exposed at the village of Zákoutí in the Orlické hory (Fig. 1). The chemical composition is given in Table 1 and by Opletal et al. (1980; Table 1, analysis 14) and corresponds to granite. The zircon population is uniformly clear to yellow-brown, long-prismatic, and idiomorphic. Eight zircons were analyzed by VTT of which one analysis is concordant and three more are discordant and well aligned along a chord through the origin with a Concordia intercept age of 509±11 Ma (Fig. 6c; Table 2). Four additional grains are more discordant and produced older $^{207}Pb/^{206}Pb$ ages between 555 and 764 Ma (not shown in Fig. 6c) which we interpret as xenocrysts. Since the same limitations apply as outlined for sample CS 6, these data can only be considered as minimum ages.

Four further grains analyzed by evaporation produced near-identical $^{207}Pb/^{206}Pb$ ratios which combine to a mean age of 511±1.1 Ma (Fig. 6c, inset; Table 3). In view of the consistency of the VTT and evaporation data, we consider the aforementioned age to most closely reflect the time of emplacement of the gneiss precursor. The $\varepsilon_{Nd(t)}$ value for whole-rock sample CS 9 is –4.0, and the mean crustal residence age is 1.5 Ga (Table 4). We offer the same interpretation as before, namely that the gneiss precursor was predominantly generated from old crust, although mixing with some juvenile material is also possible.

The granite-gneisses of the OSC intruded a sequence of felsic metavolcanics and meta-tuffs, collectively referred to as the Stronie Formation in Poland or Nové Město Group in Czechia (Opletal et al. 1980). We collected sample CS 11 from the latter, a two-mica albite schist, at a locality south of Deštné (Fig. 2), in the hope that it would contain magmatic zircons crystallized at the time of tuff formation. However, all zircons were short-prismatic in habit and had well-rounded terminations, typical of detrital grains in a sediment. Five grains analyzed by VTT were all discordant and yielded $^{207}Pb/^{206}Pb$ ages between 564±41 and 1939±5 Ma (Fig. 6d; Table 2) Two additional grains analyzed by evaporation also produced Precambrian ages of 842.1±1.7 and 1497.2±1.6 Ma, respectively (Table 3; Fig. 6d, inset). The youngest detrital zircon age of ~564 Ma (assuming that Pb-loss occurred in recent times) suggests the meta-tuff to be younger than ~564 Ma, and it contains material from a Precambrian basement that consists of Neoproterozoic and Palaeoproterozoic components. The single zircon ages obtained from sample CS 11 are in the same range as the xenocryst ages found in the granite-gneisses discussed herein. The $\varepsilon_{Nd(t)}$ value for whole-rock sample CS 11 is –3.5, and the Nd model age is 1.5 Ga (Table 4). These values support the same interpretation as advanced for the granitoid gneisses, namely that the felsic tuff was generated predominantly from old crust, and this is why only xenocrystic zircons were found in the sample analyzed.

Granite-gneiss sample CS 12 was taken from a nearby location at Zakoutí (Fig. 2) and is also of the G-type according to the Geological Map (Opletal and Domečka 1983). Its chemical composition is given in Table 1 and by Opletal et al. (1980; Table 11, analyses 9 and 15) and corresponds to granite. The zircons are predominantly clear and long-prismatic with sharp terminations, but short-prismatic grains with slightly rounded ends also occur. Evaporation of three grains of the first type produced consistent results with a mean $^{207}Pb/^{206}Pb$ age of 507.1±1.3 Ma, whereas one grain of the second type was much older at 1066.2±3.2 Ma (Fig. 5h,i; Table 3). In analogy with the previously discussed samples, we consider the younger age as reflecting the time of intrusion of the granite from which sample CS 12 was derived, whereas the older age is for a xenocryst inherited from the source of the original granite.

The $\varepsilon_{Nd(t)}$ value for whole-rock sample CS 12 is –6.5, and a mean crustal residence age of 1.7 Ga can be calculated (Table 4). The Nd isotopic data and the zircon xenocrysts again support the view that the gneiss precursor was predominantly generated from old crust.

Our next sample, CS 13, is a coarse-grained augengneiss derived from a porphyritic granite and collected in the Zdobnice Valley of the southeastern Orlické hory (Fig. 2). A second sample, CS 13 A, from the same locality, is finer grained but otherwise similar to CS 13. The chemical composition is given in Table 1 and by Opletal et al. (1980; Table 11, analyses 2, 4, and 5) and again corresponds to granite. The zircon population in both samples consists of yellow-

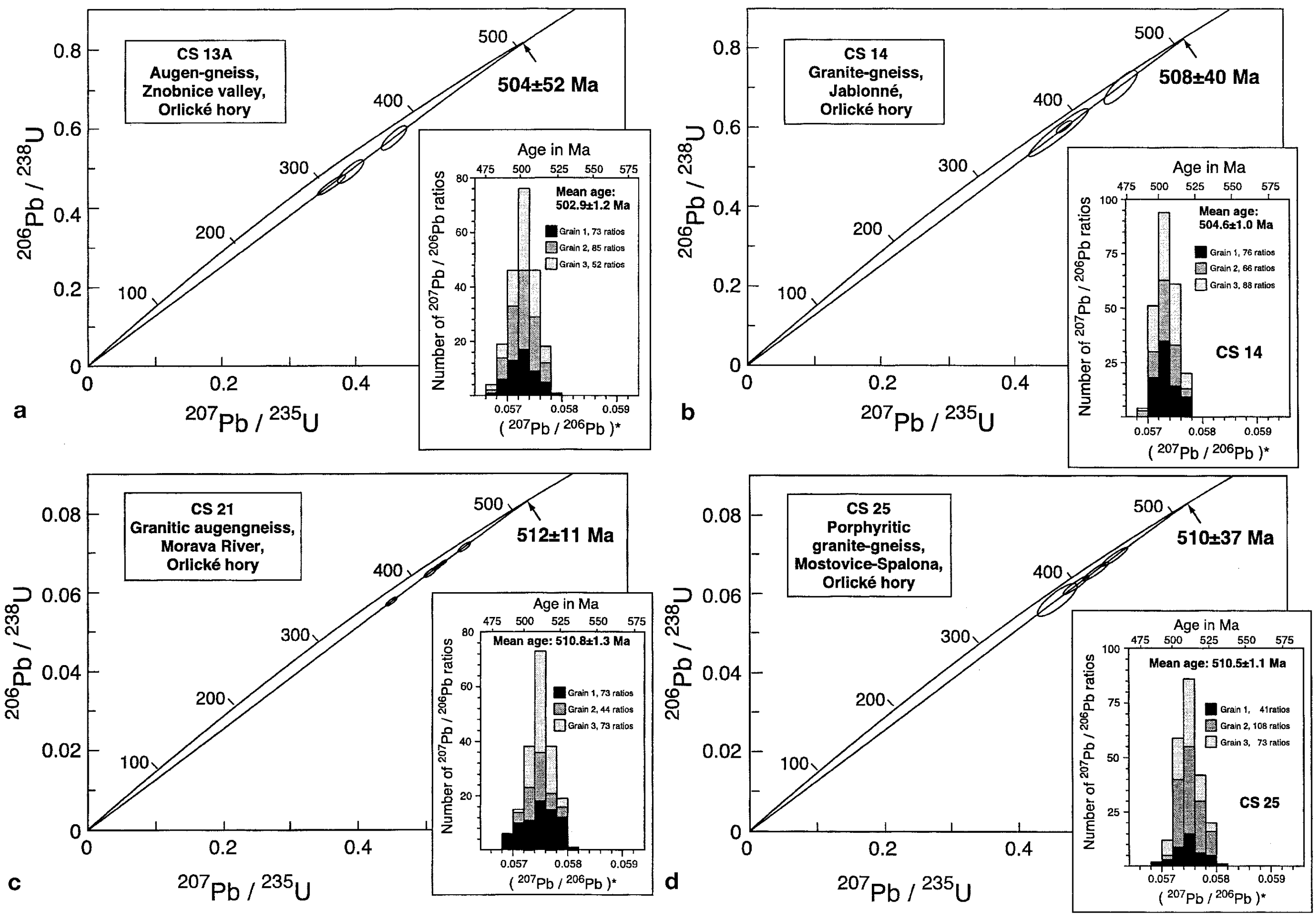

Fig. 7a–d Concordia diagrams and histograms showing analytical data for single zircons from granitic gneiss samples of the Orlické hory, Czech and Polish West Sudetes. **a** Three grains from granitic augengneiss sample CS 13A. *Inset* shows histogram with distribution of radiogenic lead isotope ratios derived from evaporation of three grains from same sample. **b** Three grains from granite-gneiss sample CS 14. *Inset* shows histogram with distribution of radiogenic lead isotope ratios derived from evaporation of three single zircons from same sample. **c** Three grains from strongly foliated augengneiss gneiss sample CS 21. *Inset* shows histogram with distribution of radiogenic lead isotope ratios derived from evaporation of four grains from same sample. **d** Four grains from porphyritic granite-gneiss sample CS 25. *Inset* shows histogram with distribution of radiogenic lead isotope ratios derived from evaporation of three grains from same sample

brown to grey-brown short-prismatic grains of which most are idiomorphic and a few have slightly rounded ends. Evaporation of three idiomorphic zircons from CS 13 yielded identical results and combine to a mean $^{207}Pb/^{206}Pb$ age of 503.5±1.1 Ma (Fig. 5j; Table 3), whereas two grains with slightly rounded terminations have older ages of 613.0±2.2 and 778.7±2.7 Ma, respectively (Fig. 5k–l; Table 3). Three additional idiomorphic grains from sample CS 13A have $^{207}Pb/^{206}Pb$ isotopic ratios virtually identical to those of zircons from sample CS 13, and their mean age is 502.9± 1.2 Ma (Fig. 7a, inset; Table 3). The combined mean evaporation age of six grains from samples CS 13 and 13A is 503.2±1.0.

Four zircons of sample CS 13A were analyzed by VTT (Table 2), and the analyses of three grains can be fitted to a chord intersecting Concordia at 504± 52 Ma (Fig. 7a), whereas one grain has a significantly older $^{207}Pb/^{206}Pb$ age of 762±17 Ma (not shown in Fig. 7a) and, like the two evaporated grains from CS 13, is interpreted as a xenocryst. As in the previous examples, we consider the good agreement between the VTT and evaporation analyses for nine grains to be indicative of the zircon population that crystallized during emplacement of the original porphyritic granite, and we adopt the more precise evaporation age of 503.2±1.0 Ma as reflecting the time of granite intrusion.

The following sample, CS 14, is also a strongly foliated granitoid augengneiss, collected east of Jablonné n.O. in the southern Orlické hory (Fig. 2), derived from a porphyritic granite. The chemical composition is given in Table 1 and is similar to Opletal et al. (1980; Table 11, analysis 1) and also corresponds to granite. The zircon population is uniformly clear to yellowish, long-prismatic and idiomorphic, and yielded identical isotopic results. Three grains were analyzed by VTT and are aligned along a chord through the origin intersecting Concordia at 508±40 Ma (Fig. 7b;

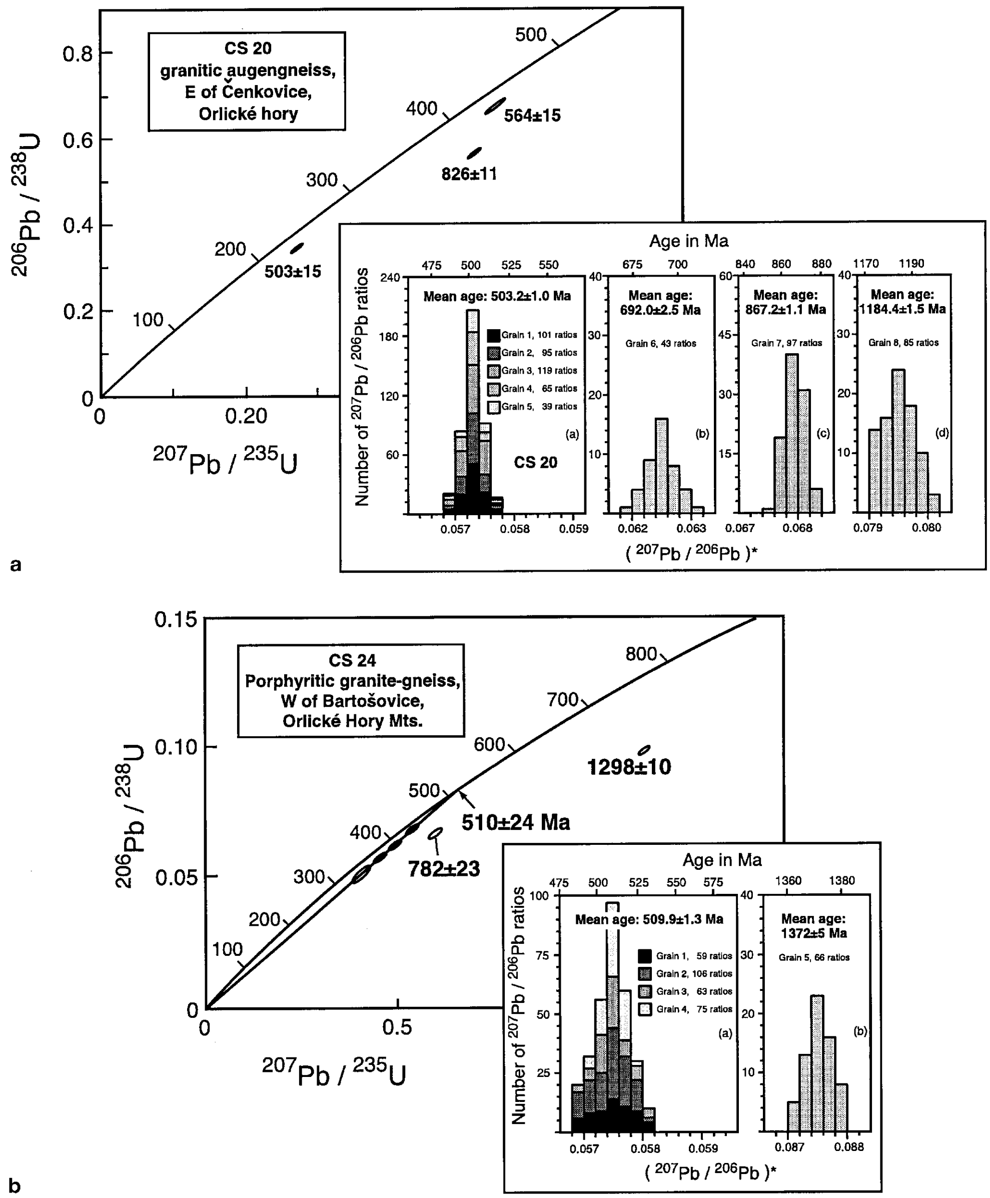

Fig. 8a,b Concordia diagrams and histograms showing analytical data for single zircons from granitic gneiss samples of the Orlické hory, Czech West Sudetes. **a** Three grains from granitic augengneiss sample CS 20. *Inset* shows histograms with distribution of radiogenic lead isotope ratios derived from evaporation of single zircons from same sample. **b** Six grains from augengneiss sample CS 24. *Inset* shows histogram with distribution of radiogenic lead isotope ratios derived from evaporation of five grains from same sample

Table 2), whereas evaporation of three grains produced a mean $^{207}Pb/^{206}Pb$ age of 504.6±1.0 Ma (Fig. 7b, inset; Table 3).

The $\varepsilon_{Nd(t)}$ value for whole-rock sample CS 14 is –6.2, and the Nd model age is 1.7 Ga (Table 4), similar as for sample CS 12. Although we found no zircon xenocrysts in this sample, it is obvious that its granitic precursor was generated from melting of older continental crust.

CS 20 is an additional example of coarse augengneiss derived by shearing of porphyritic granite and collected from near the top of the hill "Boková" SE of Čenkovice in the southern Orlické hory (Fig. 2). The chemical composition is given in Table 1 and is similar to that of Opletal et al. (1980; Table 11, analysis 1) and corresponds to granite. The zircons are again clear and long-prismatic with occasional slight rounding at their terminations. Three grains were analyzed by VTT (Table 2) and all are discordant (Fig. 8a). Only one grossly discordant grain yielded a minimum $^{207}Pb/^{206}Pb$ age of 503±15 Ma, comparable to that of the previous samples. The other two grains have minimum ages of 564±15 and 826±11 Ma, respectively, and are probably xenocrysts. Eight grains were evaporated (Table 3), five were idiomorphic, and the remaining three had slightly rounded ends. The idiomorphic variety produced consistent $^{207}Pb/^{206}Pb$ ratios combining to a mean age of 503.2±1.0 Ma which we consider to reflect the age of emplacement of the gneiss precursor. The slightly rounded, xenocrystic grains yielded ages of 692.0±2.5, 867.2±1.1, and 1184.4±1.5 Ma, respectively (Fig. 8a, inset) and reflect a heterogeneous Precambrian basement below the Orlické hory.

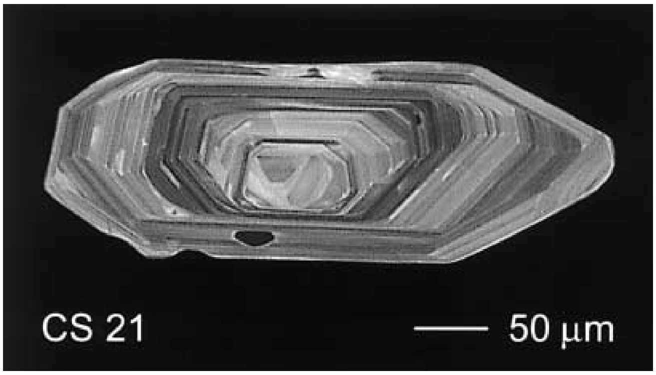

Fig. 9 Cathodoluminescence photograph of typical zircon grain from sample CS 21 showing oscillatory zoning typical of magmatic growth. This type of internal structure is typical of almost all grains analyzed in this study

The $\varepsilon_{Nd(t)}$ value for whole-rock sample CS 20 is –4.8, and the Nd model age is 1.6 Ga (Table 4). These values are in the same range as those for the other granitoid gneisses presented thus far, and we offer a similar interpretation, i.e., generation of the original granite from melting of older crust.

Two additional samples were collected in the Sněžník Mountains, one in Czechia and one in Poland. Sample CS 21 is an augengneiss also derived from a coarse, porphyritic granite and occurs in the southern part of the Sněžník Mountains in the Morava River east of the town of Králíky and approximately 1 km ENE of the village of Vysoký Potok (Fig. 1). This rock, like almost all previous samples, chemically corresponds to granite (Table 1). The zircons are clear to yellowish and idiomorphic and, like virtually all other magmatic grains of this study, show well-developed oscillatory zoning under cathodoluminescence (Fig. 9). Five grains were analyzed by VTT (Table 2), and the data are well aligned along a chord through the origin intersecting Concordia at 512±11 Ma (Fig. 7c). Evaporation of three additional grains yielded the same results, and the data can be combined to a mean $^{207}Pb/^{206}Pb$ age of 510.8±1.3 Ma (Fig. 7c, inset; Table 3). No xenocrysts were encountered in this sample.

The $\varepsilon_{Nd(t)}$ value for whole-rock sample CS 21 is –3.9, and the Nd model age is 1.5 Ga (Table 4). Again, these values are within the range of the other samples and, therefore, the same genetic interpretation applies.

Sample CS 24 is a very coarse augengneiss with a pronounced stretching lineation. This rock, collected in a small quarry west of Bartoäovice (Fig. 2), is inhomogeneously deformed with the least deformed layers consisting of porphyritic granite with slight alignment of feldspar phenocrysts, whereas some layers are intensely sheared and almost mylonitized. Most zircons are clear to pink, long-prismatic, and almost completely idiomorphic, whereas a minority of grains is clear to light yellow with distinct rounding at the pyramidal terminations. Six grains were analyzed by VTT (Table 2) of which four were of the idiomorphic variety and yielded discordant results that are well aligned along a regression line through the origin (MSWD=0.005) with an upper Concordia intercept at 510±24 Ma (Fig. 8b). Two additional grains with rounded terminations are strongly discordant and have $^{207}Pb/^{206}Pb$ minimum ages of 782±23 and 1298±10 Ma, respectively (Table 2, Fig. 8b). Four additional idiomorphic grains were evaporated and produced a mean $^{207}Pb/^{206}Pb$ age of 509.9±1.3 Ma, whereas an additional grain with rounded ends is much older at 1372±5 Ma (Fig. 8b, inset; Table 3). We interpret the age of ~510 Ma as reflecting the time of emplacement of the porphyritic granite from which the augengneiss was derived. The older grains are seen as components of a Precambrian basement from which the magma of the porphyritic granite was derived by anatexis or through which it was emplaced.

Sample CS 25 is a coarse-grained granitic augengneiss collected in a small quarry at the village of Mostowice-Spalona in the Polish part of the Orlické hory, known in Poland as Góry Bystrzyckie (Fig. 2). The zircons are long, clear and idiomorphic, typical of magmatic growth. Four grains were analyzed by VTT and produced slightly discordant (Table 2) but reasonably well-aligned results with an imprecise upper Concordia intercept age of 510±37 Ma (Fig. 7d). Three additional grains were evaporated and yielded a much better defined mean $^{207}Pb/^{206}Pb$ age of 510.5±1.1 Ma (Fig. 7d, inset; Table 3) which we interpret as reflecting the time of emplacement of the gneiss precursor. This age is identical to that of augengneiss sample CS 24.

Lastly, we analyzed sample CS 72 from a 10-m-wide undeformed amphibole–biotite microgranite dyke which cuts foliated granitoid orthogneiss in an abandoned quarry near the village of Zdobnice (Fig. 2). This dyke belongs to a suite of microgranitic to lamprophyric rocks which are widespread in the Orlické hory and were described in detail by Opletal (1980) who considered them as late- to post-orogenic (pre-Variscan, probably Caledonian) with respect to the deformation in the host rocks. The idiomorphic zircons are clear to pale yellow and stubby to long-prismatic. Six grains were evaporated and yielded consistent $^{207}Pb/^{206}Pb$ ratios with a mean age of 491.7±1.0 Ma (Fig. 5m; Table 3). This age is very significant since it demonstrates that the foliation in the adjacent orthogneisses must be older than ~492 Ma and is therefore pre-Variscan, as suggested by Opletal (1980) and Přikryl et al. (1996).

Discussion and conclusion

Our new ages are in good agreement with U–Pb zircon ages reported by Oliver et al. (1993) and document a chronologically and chemically unusually

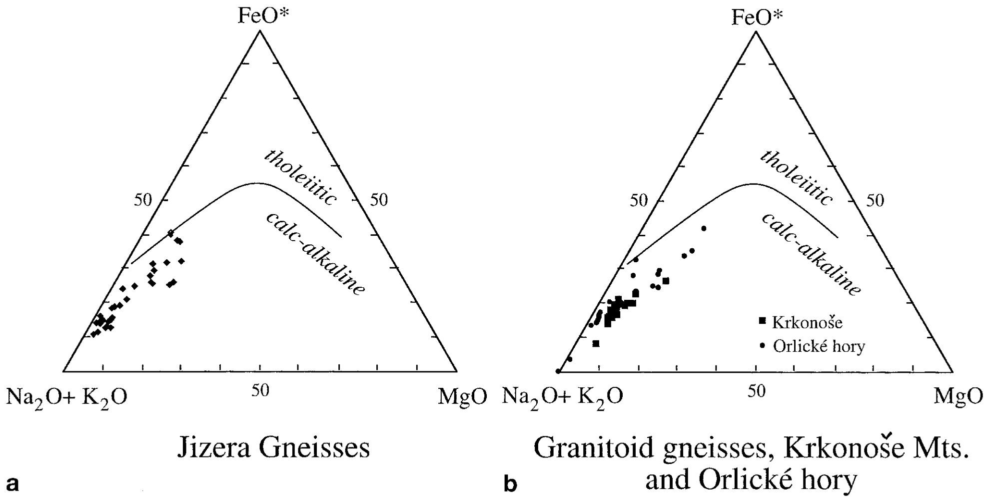

Fig. 10a,b AFM plots for granitoid orthogneisses from **a** the Jizerské hory and **b** the Krkonoše Mountains and Orlické hory showing calc-alkaline trends. Data source: Domečka (1970); Opletal et al. (1980); and Table 1. Boundary between calc-alkaline and tholeiitic fields after Irvine and Baragar (1971)

homogeneous granitoid province of Cambrian age in the Czech Sudetes extending from the Jizera Mountains in the NW to the Orlické-Sněžník Complex in the SE. Magmatic and metamorphic ages around 500–505 Ma were also recorded in the Staré Město belt farther E (Kröner et al., 2000) along which the Lugian domain containing the OSC was overthrust over the Silesian Domain containing the Desná and Keprník domes (Schulmann and Gayer 2000).

The structural and metamorphic history of the OSC as documented by Přikryl et al. (1996) and Cymerman (1997) is, however, *not* recorded in our zircon ages. Nevertheless, we tentatively conclude on the basis of ~440- to 463-Ma zircon ages for migmatitic and anatectic rocks in the Góry Sowie Mountains of the Polish Sudetes (Oliver et al. 1993; Kröner and Hegner 1998) and the Cambrian ages for granulite-facies assemblages in the Staré Město belt (Kröner et al., 2000) that at least the early deformational/metamorphic event (generation of first foliation in the gneisses, tight folding, migmatization, and associated high-temperature conditions and anatexis) is of early Palaeozoic age. This is in accord with field relationships (Opletal et al. 1980; Don et al. 1990; Přikryl et al. 1996), and the age of 492 Ma for our micrograniteldyke sample CS 72 also supports this interpretation. It is likely that the Rb–Sr whole-rock cooling ages of 462–487 Ma for the Jizera and Sněžník gneisses (Borkowska et al. 1980; Van Breemen et al. 1982) also reflect this event. This implies that an important part of the orogenic history of the West Sudetes is pre-Variscan in age, in contrast to the interpretation of Alexandrowski et al. (2000).

The orthogneisses in the West Sudetes are predominantly of granitic composition, but there are also granodiorites and, more rarely, trondhjemites and tonalites (Domečka 1970; Opletal et al. 1980, see also Table 1). Figure 10 shows AFM plots of the Izera gneisses (data from Domečka 1970) and the granitoid gneisses of the Krkonoše Mountains and Orlické hory (data from Table 1 and Opletal et al. 1980) and demonstrates the calc-alkaline trend for these rocks. This is further underlined by the trace element discrimination diagram of Fig. 11 (data from Table 1) where all rocks discussed in this paper as well as those previously reported from the Góry Sowie in the Polish part of the West Sudetes (Kröner and Hegner 1998) plot in the field of volcanic arc and syn-collisional granites (Pearce et al. 1984). Similar geochemical features were reported by Turniak et al. (2000) for the Sněžník and Gierałtow gneisses in Poland. Based on the overall chemical evidence, the ~500-Ma West Sudetes granitoid gneisses show little resemblance to granite associations typically confined to late- to post-collisional or within-plate settings. They are chemically similar to orogenic granite suites and therefore lend support to a subduction-related origin.

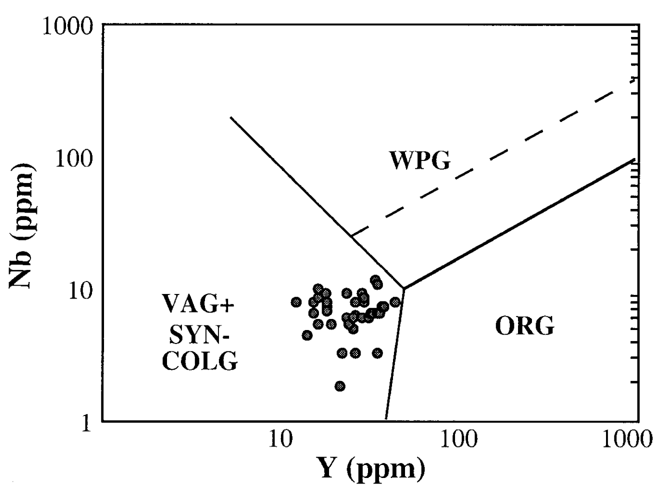

Fig. 11 Nb vs Y trace element discrimination diagram (after Pearce et al. 1984) showing position of granitoid orthogneisses from Czech West Sudetes (data from Table 1) and Gory Sowie, Polish West Sudetes (data from Kröner and Hegner 1998). *VAG* volcanic arc granites; *SYN-COLG* syn-collisional granites; *ORG* orogenic granites; *WPG* Within-plate granites

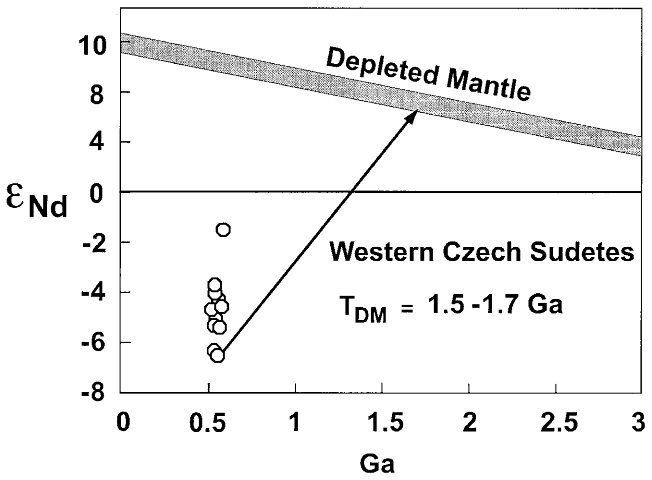

Fig. 12 Nd isotopic evolution diagram for whole-rock samples of granitic gneisses from the Czech West Sudetes. Data from Table 4. *Arrow* shows evolution of the $^{143}Nd/^{144}Nd$ ratio for sample CS 12

Initial ε_{Nd} values for the orthogneisses show a range between –3.5 (CS 11) and –6.5 (CS 12; Fig. 12; Table 4) and mean crustal residence ages between 1.5 and 1.7 Ga. There is a fair correlation between $\varepsilon_{Nd(t)}$ values and the presence of zircon xenocrysts in most samples, and we see a direct relationship between zircon xenocryst ages and Nd model ages. However, our age range for the xenocrysts may not necessarily be representative for each sample and, in any case, the xenocrysts provide *minimum* ages for the source region of their host rocks.

Kröner and Hegner (1998) suggested on the basis of chemical data and Nd isotopic systematics that the Góry Sowie granitoids are calc-alkaline in character and constituted part of an Andean-type magmatic arc of Eastern Avalonia that evolved during Ordovician closure of the Tornquist ocean. Our new data from the Czech part of the West Sudetes substantiate this model but suggest that arc formation in the Jizerské hory-Krkonoše-Orlické hory segment of the West Sudetes was slightly earlier and occurred in Cambrian times. Furthermore, abundant evidence for xenocrystic zircons in the dated orthogneisses as well as the distinctly negative $\varepsilon_{Nd(t)}$-values suggest extensive melting of Precambrian continental basement in the generation of the granitic gneiss precursors (Hegner and Kröner, 2000). This basement, as typified by our xenocryst ages, is not characteristic of North Africa (Cahen et al. 1984), from where most parts of the Bohemian Massif are supposed to be derived. Crust with ages in the range 1000–1400 Ma is unknown from this region but has been reported from northwestern Venezuela and northern Colombia (Kroonenberg 1982; Priem et al. 1989; Restrepo-Pace et al. 1997; Ruiz et al. 1999) as part of the Grenville mobile belt which extended from northwestern Canada via Mexico to as far south as Peru and northern Argentina (Dalziel et al. 1994). Possible scenarios which suggest derivation of the West Sudetes from the northwestern margin of Gondwana are further discussed by Kröner et al. (2000) and Hegner and Kröner (2000).

We therefore reiterate previous speculations (Oliver 1996; Kröner and Hegner 1998) that the West Sudetes belong to eastern Avalonia which was probably rifted off the northern Guyana shield in latest Precambrian time (see also discussion in Hegner and Kröner, 2000). This Avalonia superterrane then drifted towards Baltica in Cambrian and Ordovician times and developed an active margin on its Baltica-facing side, along which accretionary wedges and subduction-related granitoids were formed and immediately deformed after their generation. Crustal thickening during this accretion/amalgamation process led to widespread regional metamorphism shortly after 500 Ma as documented by Přikryl et al. (1996) and our age of ~492 Ma for a cross-cutting microgranite dyke in the Orlické hory. Finally, our data support the concept of a Caledonian orogeny in the West Sudetes (Johnston et al. 1994), although much of the evidence was obliterated during the Variscan event.

Acknowledgements Financial support to A.K. and E.H. by the Deutsche Forschungsgemeinschaft (DFG) within the Priority Program "Orogenic Processes" (grant nos. Kr 590/35 and He 1857/4) is gratefully acknowledged. A.K. also appreciates mass spectrometer analytical facilities in the Max-Planck-Institut für Chemie in Mainz. We thank K. Schulman, P. Štipská, Z. Cymermann, A. Żelaźniewicz, S. Mazur, and J. Don for discussions in the field, and G. Oliver, J. Janoušek, and K. Schulmann for careful reviews. This is a contribution to EUROPROBE.

References

Alexandrowski P, Kryza R, Mazur S, Pin C, Zalasiewicz JA (2000) The Polish Sudetes: Caledonian or Variscan? Trans R Soc Edinburgh Earth Sci 90:127–146

Arndt NT, Goldstein SL (1987) Use and abuse of crust-formation ages. Geology 15:893–895

Bakun-Czubarow N (1992) Quartz pseudomorphs after coesite and quartz evolution in eclogitic omphacites of the Złote Mountains in the Sudetes (SW Poland). Arch Mineral 48:3–25

Bakun-Czubarow N (1993) Recent data on isotope geochronology of metamorphic rocks of the Orlica-Snieznik dome. Europrobe meeting in Loučná, abstract vol, Charles Univ, Prague, pp 3–5

Bederke E (1925) Bau und Alter des ostsudetischen Gebirges. N Jahrb Mineral Geol Paläontol Abt B Beil-Band 53:98–116

Bederke E (1929) Die Grenze von Ost- und Westsudeten. Geol Rundsch 20:186–205

Bederke E (1939) Die kaledonische Gebirgsbildung in Mitteleuropa. Z Dtsch Geol Ges 91:770–771

Bederke E (1943) Ein Profil durch das Grundgebirge der Grafschaft Glatz. Geol Rundsch 34:6–9

Bederke E (1956) Das Alter des moldanubischen Grundgebirges. Geol Rundsch 45:167–175

Borkowska M, Dörr W (1998) Some remarks on the age and mineral chemistry of orthogneisses from the Ladek-Snieznik metamorphic massif, Sudetes, Poland. Terra Nostra 98:27–30

Borkowska M, Hameurt J, Vidal P (1980) Origin and age of Izera gneisses and Rumburk granites in the Western Sudetes. Acta Geol Polon 30:121–146

Borkowska M, Choukroune P, Hameurt J, Martineau F (1990) A geochemical investigation of the age, significance and structural evolution of the Caledonian–Variscan granite-gneisses of the Śnieżnik metamorphic area (Central Sudetes, Poland). Geol Sudet 25:1–27

Cahen L, Snelling NJ, Delhal J, Vail JR (1984) The geochronology and evolution of Africa. Clarendon Press, Oxford

Chaloupský J (ed) (1989) Synoptic geological map of the Krkonoše and Jizerské Hory Mountains, 1:100,000. Geological Survey Czechoslovakia, Prague

Cocherie A, Guerrot C, Rossi PH (1992) Single-zircon dating by stepwise Pb evaporation: comparison with other geochronological techniques applied to the Hercynian granites of Corsica, France. Chem Geol 101:131–141

Cymerman Z (1992) Rotation ductile deformation in the Śnieżnik metamorphic complex. Kwartalnik Geol 36:394–420

Cymerman Z (1997) Structure, kinematics and evolution of the Orlica-Śnieżnik dome, Sudetes. Prace Panstwowego Inst Geol 156:1–120

Cymerman Z, Piasecki MAJ, Seston R (1997) Terranes and terrane boundaries in the Sudetes, northeast Bohemian Massif. Geol Mag 134:717–725

Dalziel IWD, Dalla Salda LH, Gahagan LM (1994) Paleozoic Laurentia–Gondwana interaction and the origin of the Appalachian–Andean mountain system. Geol Soc Am Bull 106:243–252

Dörr W, Fiala J, Vejnar Z, Zulauf G (1998) U–Pb ages and structural development of metagranitoids of the Teplá crystalline complex: evidence for pervasive Cambrian plutonism within the Bohemian massif (Czech Republic). Geol Rundsch 87:135–149

Domečka K (1970) Pre-Variscan granitoids of the West Sudeten. Sborník Geol Věd Geol 18:161–191 (in Czech with English summary)

Don J (1964) Góry Zlote i Krowiarki jako elementy skladove metamorfiku Śnieżnika. Geol Sudet 1:79–117

Don J, Opletal M (1996) Budowa i ewolucja geologiczna Masywu Snieżnika. In: Jahn A, Kozłowski S, Pulina M (eds) Masyw Snieýnika – zmiany w srodowisku pryrodniczym. Polska Agencja Ekologiczna, Warsaw, pp 13–26

Don J, Dumicz M, Wojciechowska I, Żelaźniewicz A (1990) Lithology and tectonics of the Orlica-Śnieżnik Dome, Sudetes: recent state of knowledge. N Jahrb Geol Paläontol Abh 179:159–188

Dumicz M (1979) Tectogenesis of the metamorphosed series of the Klodzko district: a tentative explanation. Geologica Sudetica 14:29–46

Dumicz M (1991) Relation betwen eclogites and Midzygórze gneiss unit by structural analysis. Acta Universitatis Wratislawiences, 1276, Prace Geol Miner 19:31–46 (in Polish)

Fischer G (1935) Der Bau des Glatzer Schneegebirges. Jahrb Preuss Geol Landesanst 56:712–732

Gastil RG, De Lisle M, Morgan JR (1967) Some effects of progressive metamorphism on zircons. Geol Soc Am Bull 78:879–906

Hegner A, Kröner A (2000) Review of Nd isotopic data and xenocrystic and detrital zircon ages from the pre-Variscan basement in the eastern Bohemian Massif: speculations on palinspastic reconstructions. Geol Soc Lond Spec Publ 179:113–130

Hegner E, Watter HJ, Satir M (1995) Pb–Sr–Nd isotopic compositions and trace element geochemistry of megacrysts and melililites from the Tertiary Urach volcanic field: source composition of small-volume melts under SW Germany. Contrib Mineral Petrol 122:322–335

Irvine TN, Baragar WRA (1971) A guide to the chemical classification of the common volcanic rocks. Can J Earth Sci 8:523–548

Jaeckel P, Kröner A, Kamo SL, Brandl G, Wendt JI (1997) Late Archaean to early Proterozoic granitoid magmatism and high-grade metamorphism in the central Limpopo belt, South Africa. J Geol Soc Lond 154:25–44

Johnston JD, Tait JA, Oliver GJH, Murphy FC (1994) Evidence for a Caledonian orogeny in Poland. Trans R Soc Edinburgh Earth Sci 85:131–142

Karabinos P (1997) An evaluation of the single-grain zircon evaporation method in highly discordant samples. Geochim Cosmochim Acta 61:2467–2474

Kober B (1986) Whole-grain evaporation for $^{207}Pb/^{206}Pb$-age-investigations on single zircons using a double-filament thermal ion source. Contrib Mineral Petrol 93:482–490

Kober B (1987) Single-zircon evaporation combined with Pb^+ emitter-bedding for $^{207}Pb/^{206}Pb$-age investigations using thermal ion mass spectrometry, and implications to zirconology. Contrib Mineral Petrol 96:63–71

Korytowski A, Dörr W, Żelaźniewicz A (1993) U–Pb dating of (meta)granitoids in the NW Sudetes (Poland) and their bearing on tectono-stratigraphic correlations. Terra Abstr 5:331–332

Kozłowska-Koch M (1965) The granite-gneiss of the Izera Highlands. Arch Mineral 25:123–259

Krogh TE (1978) Vapour transfer for the dissolution of zircons in a multi-sample capsule at high pressure. US Geol Surv Open-File Rep 78-701:233–234

Kröner A, Hegner E (1998) Geochemistry, single zircon ages and Sm-Nd systematics of granitoid rocks from the Góry Sowie (Owl) Mountains, Polish West Sudetes: evidence for early Paleozoic arc-related plutonism. J Geol Soc Lond 155:711–724

Kröner A, Todt W (1988) Single zircon dating constraining the maximum age of the Barberton greenstone belt, southern Africa. J Geophys Res 93:15329–15337

Kröner A, Byerly GR, Lowe DR (1991) Chronology of early Archaean granite-greenstone evolution in the Barberton Mountain Land, South Africa, based on precise dating by single zircon evaporation. Earth Planet Sci Lett 103:41–54

Kröner A, Hegner E, Hammer J, Haase G, Bielicky K-H, Krauss M, Eidam J (1994a) Geochronology and Nd–Sr systematics of Lusatian granitoids: significance for the evolution of the Variscan orogen in east-central Europe. Geol Rundsch 83:357–376

Kröner A, Jaeckel P, Williams IS (1994b) Pb-loss patterns in zircons from a high-grade metamorphic terrain as revealed by different dating methods: U–Pb and Pb–Pb ages for igneous and metamorphic zircons from northern Sri Lanka. Precambrian Res 66:151–181

Kröner A, Willner AP, Hegner E, Frischbutter A, Hofmann J, Bergner R (1995) Latest Precambrian (Cadomian) zircon ages and Nd isotopic systematics and P–T-evolution of granitoid orthogneisses of the Erzgebirge, Saxony and Czech Republic. Geol Rundsch 84:437–456

Kröner A, Jaeckel P, Brandl, G., Nemchin AA, Pidgeon RT (1999) Single zircon ages for granitoid gneisses in the Central Zone of the Limpopo belt, southern Africa, and geodynamic significance. Precambrian Res 93:299–337

Kröner A, Štípská P, Schulmann K, Jaeckel P (2000) Chronological constraints on the pre-Variscan evolution of the northeastern margin of the Bohemian Massif, Czech Republic. In: Franke W, Altherr R, Haak V, Oncken O, Tanner D (eds) Orogenic processes: quantification and modelling in the Variscan belt of central Europe. Geol Soc Lond Spec Publ 179:175–198

Kroonenberg SB (1982) A Grenvillian granulite belt in the Colombian Andes and its relation to the Guiana shield. Geol Mijnb 61:325–333

Laskowski N, Kröner A (1985) Geochemical characteristics of Archaean and late Proterozoic to Paleozoic fine-grained sediments from southern Africa and significance for the evolution of the continental crust. Geol Rundsch 74:1–9

Liew TC, Hofmann AW (1988) Precambrian crustal components, plutonic associations, plate environment of the Hercynian Fold Belt of Central Europe: indications from a Nd and Sr isotopic study. Contrib Mineral Petrol 98:129–138

Mísař Z (1963) Předdevonský geologický vývoj sv. okraje Českého masívu. Rozpr Čs Akad Věd, Ř mat přír Věd 73:1–60
Mísař Z, Dudek A, Havlena V, Weiss J (1983) Geology of the Czech Republic. I. Czech Massif. Státní pedagogické nakladatelství, Prague (in Czech)
Oberc J (1961) An outline of the geology of the Karkonosze-Izera Block. Zesz Nauk Uniw Nauki Przyr, Warsaw, Ser B:139–170
Oberc J (1969) Geology of the Sudetes Mountains. Prace Institutu Geologicznego, 30, 2, Wydawnictwo Geologiczne Warszawa (in Polish)
Oberc J (1972) Budowa geologiczna Polski, IV. Tektonika. 2. Sudety i obszary przylegle. Wydaw Geol Warzaw
O'Connor JT (1965) A classification for quartz-rich igneous rocks based on feldspar ratios. US Geol Surv Prof Pap B525:79–84
Oliver GJH (1996) Geochronology of the Western Sudetes, Poland: the controversial period from 550 to 350 Ma. Abstract volume, EUROPROBE TESZ Workshop, Ksiaz, Poland
Oliver GJH, Corfu F, Krogh TE (1993) U–Pb ages from SW Poland: evidence for a Caledonian suture zone between Baltica and Gondwana. J Geol Soc Lond 150:355–369
Opletal M (1997) Genesis of orthogneisses of the Orlice-Sněžník unit). DSc thesis, Univ Brno (in Czech with English summary)
Opletal M et al. (1980) Geologie Orlických hor (Geology of the Orlické hory). Geological Survey, Prague (in Czech with extended English summary)
Opletal M, Domečka K (eds) (1983) Synoptic geological map of the Orlické Hory Mountains, 1:100,000. Geological Survey of Czechoslovakia, Prague
Parrish RR (1987) An improved microcapsule for zircon dissolution in U–Pb geochronology. Chem Geol 66:99–102
Pearce JA, Harris NBW, Tindle AG (1984) Trace element discrimination diagrams for the tectonic interpretation of granitic rocks. J Petrol 25:956–983
Philippe S, Haack U, Żelaźniewicz A, Dörr W, Franke W (1995) Preliminary geochemical and geochronological results on shear zones in the Izera-Karkonosze Block (Sudetes, Poland). Terra Nostra 95:122
Priem HNA, Kroonenberg SB, Boelrijk NAIM, Hebeda EH (1989) Rb–Sr and K–Ar evidence for the presence of a 1.6 Ga basement underlying the 1.2 Ga Garzón-Santa Marta granulite belt in the Colombian Andes. Precambrian Res 42:315–324
Přikryl R, Schulmann K, Melka R (1996) Perpendicular fabrics in the Orlické hory orthogneisses (western part of the Orlice-Sněžník Dome, Bohemian Massif) due to high temperature E–W deformational event and late lower temperature N–S overprint. J Czech Geol Soc 41:156–166
Restrepo-Pace PA, Ruiz J, Gehrels G, Cosca M (1997) Geochronology and Nd isotopic data of Grenville-age rocks in the Colombian Andes: new constraints for late Proterozoic–early Paleozoic paleocontinental reconstructions of the Americas. Earth Planet Sci Lett 150:427–441
Ruiz J, Tosdal RM, Restrepo PA, Murrillo-Muñetón G (1999) Pb isotope evidence for Colombia-southern Mexico connection in the Proterozoic. In: Ramos V, Keppie JD (eds) Laurentia–Gondwana connections before Pangaea. Geol Soc Am Spec Pap 336:183–198
Schulmann K, Gayer R (2000) A model for a continental accretionary wedge developed by oblique collision: the NE Bohemian Massif. J Geol Soc Lond 157:401–416
Schwarzbach M (1943) Vulkanismus und Senkung in der kaledonischen Geosynklinale Mitteleuropas. Geol Rundsch 34:13–34
Silver LT (1969) A geochronological investigation of the anorthosite complex, Adirondack Mountains, New York. In: Isachsen YW (ed) Origin of anorthosite and related rocks. NY Museum Sci Service Mem 18:57–82
Smulikowski K (1979) Ewolucja polimetamorficzna krystaliniku u Śnieznika Klodzkiego i Gór Zlotych w Sudetach. Geol Sudet 14:7–76 (in Polish with English summary)
Stacey JS, Kramers JD (1975) Approximation of terrestrial lead isotope evolution by a two-stage model. Earth Planet Sci Lett 26:207–221
Suess FE (1912) Die moravischen Fenster und ihre Beziehung zum Grundgebirge des Hohen Gesenkes. Denkschr Österr Akad Wiss Math-Naturwiss Kl 88:541–631
Suk M. et al. (1984) Geological history of the territory of the Czech Socialist Republic. Ústřední ústav Geologický, Prague
Svoboda J et al. (1966) Regional geology of Czechoslovakia. Part I. The Bohemian Massif. Ostřední ústav geologický, Prague (in Czech)
Szałamacha M, Szałamacha J (1964) Northern contact of micaceous schists of the Kamienica belt with the Izerskie gneisses. Przegl Geol 7:329–331
Teisseyre JH (1973) Metamorphosed rocks of Rudawy Janowickie i Grzbiet Lasocki Mountains Geol Sudet 8:7–110
Turniak K, Mazur S, Wysoczaäski R (2000) SHRIMP zircon geochronology and geochemistry of the Orlica-Snieznik gneisses (Sudetes, SW Poland) and implications for the evolution of the Variscides in east-central Europe. Geodyn Acta 13:293–312
Van Breemen O, Aftalion M, Bowes DR, Dudek A, Mísař Z, Povondra P, Vrána S (1982) Geochronological studies of the Bohemian Massif, Czechoslovakia, and their significance in the evolution of Central Europe. Trans R Soc Edinburgh Earth Sci 73:89–108
Watznauer A (1955) Saxothuringium-Lugikum, ein regionaltektonischer Vergleich. Freiberg Forschung C17:30–53
Wendt JI (1993) Early Archean crustal evolution in Swaziland, southern Africa, as revealed by combined use of zircon geochronology, Pb–Pb and Sm–Nd systematics. Doctoral dissertation, Univ Mainz, Germany, 123 pp
Wendt JI, Todt W (1991) A vapour digestion method for dating single zircons by direct measurement of U and Pb without chemical separation. Terra Abstr 3:507–508
York D (1969) Least squares fitting of a straight line with correlated errors. Earth Planet Sci Lett 5:320–324
Żaba J (1984) Some remarks on pre-Variscan contact metamorphism of rocks of the Izera block (western Sudetes). Bull Polish Acad Sci Earth Sci 32:73–80
Żelaźniewicz A (1997) The Sudetes as a Paleozoic orogen in central Europe. Geol Mag 134:691–702
Żelaźniewicz A, Achramowicz S Nowak I, Lorenc MW (1998) Northern Izera-Karkonosze Block: a mode of Variscan reworking of Neoproterozoic (Cadomian?) continental crust. Terra Nostra 98:172–174